Au-Ag tellurides and sulphosalts from epithermal Au-Ag-Pb-Zn-Cu deposit Banská Hodruša at the Rozália mine (Slovakia)

Martin Chovan[1], Alexander Kubač[2], Tomáš Mikuš[3], Peter Žitňan[4] & Ján Prcúch[5]

[1] Department of Mineralogy and Petrology, Faculty of Natural Sciences, Comenius University, Ilkovičova 6, 542 15 Bratislava, Slovakia
[2] Department of Geology of Minerals Deposits, Faculty of Natural Sciences, Comenius University, Ilkovičova 6, 542 15 Bratislava, Slovakia
[3] Earth Science Institute of the Slovak Academy of Sciences, Ďumbierska 1, 974 01 Banská Bystrica, Slovakia
[4] Slovenské Kovy, Ltd., Kammerhofská 8, 969 01 Banská Štiavnica, Slovakia
[5] Slovenská Banská, Ltd., 966 61 Hodruša-Hámre 388, Slovakia

AGEOS

Abstract: The Au-Ag-Pb-Zn-Cu epithermal deposit Banská Hodruša of intermediate-sulphidation type is located in the middle Miocene Štiavnica Stratovolcano on the inner side of the Carpathian arc in Slovakia. There are two different styles of epithermal mineralization within the deposit. The earliest represents a subhorizontal multi-stage vein system (low-angle normal shear zone), while the much younger mineralization represents the extensive system of steep-dipping veins related to different tectono-geological events. Within the mineralization related to the shear zone the mineral Au-Ag-Te-S assemblage was determined, represented by zonal gold/electrum, hessite, petzite, Cu-cervelleite, and Te-polybasite, all associate with galena. The altaite and unnamed AgPbTeS phase were found in hessite. Very rare zonal gold/electrum crystallized to quartz vugs, with Ag content ranging from 17.8 to 45.3 wt. %. Similar assemblage was determined in flotation concentrates from dressing plant, represented by Au-Ag tellurides calaverite-krennerite-sylvanite in association with hessite, Au-hessite, petzite, unnamed AgAuTeS phase, uytenbogaardtite, and petrovskaite. These minerals typically occur in form of aggregates or as thin rims around gold/electrum. The younger horst-related veins host Ag-(Bi, Cu, Sb, As)-S assemblage. The main mineral in this assemblage is polybasite-pearceite, the other minerals jalpaite, matildite, acanthite, schapbachite, cervelleite, and arcubisite are rare and typically associate with galena. Zonal aggregates of tetrahedrite-tennantite were found in association with base metal sulphides.

Key words: epithermal mineralization, tellurides, sulphosalts, gold, Rozália mine, Hodruša-Hámre, Štiavnica Stratovolcano

1. INTRODUCTION

Tellurides and sulphosalts of Au, Ag, Pb and other base metals commonly occur as trace minerals in magmatic-hydrothermal mineral deposits, especially in epithermal gold deposits of low- to intermediate-sulphidation type associated with alkaline to calc-alkaline magmatism (Sillitoe, 2002; Ciobanu et al., 2006). Electrum, acanthite, Ag-sulphosalts, Ag-selenides, and Au-Ag tellurides are the main Au- and Ag-bearing minerals (Simmons et al., 2005). A various minerals of Au-Ag-Te system (e.g., hessite, petzite, sylvanite, krennerite) were found in some famous deposits of the Carpathian arc, such as Roşia Montană, Baia Mare, and Săcărâmb in Romania (cf. Alderton & Fallick, 2000; Grancea et al., 2002; Wallier et al., 2006; Cook et al., 2004) and Banská Štiavnica (Jeleň & Háber, 2000; Jeleň et al., 2004; Majzlan et al., 2016). These deposits display similarities with other deposits worldwide e.g., Golden Mile, Australia (Shackleton et al., 2003); Cripple Creek and Golden Sunlight, USA (Spry et al., 1997); Emperor, Fiji (Pals & Spry, 2003); Acupan and Baguio, Philippines (Cooke & McPhail, 2001). Au-Ag minerals are developed mostly on steeply-dipping veins where they are associated with gold/electrum and base metal sulphides, typically pyrite, chalcopyrite, galena, and sphalerite (Simmons et al., 2005).

The intermediate-sulphidation precious and base metal deposit Banská Hodruša (Koděra et al., 2005) occurs within the Štiavnica-Hodruša ore district in the central zone of the large middle Miocene Štiavnica Stratovolcano. The district is one of the largest ore districts in the Carpathian arc, famous for Au-Ag mining of epithermal veins of intermediate- to low-sulphidation type since the Middle Ages (e.g., Koděra & Lexa, 2010; Bakos et al., 2017; Majzlan et al., 2018). There are two styles of epithermal mineralization at the deposit, each with different structural controls, mineralogy, genetical aspects, and ages. The earlier mineralization (actually mined) represents a complex multi-stage system with unusual subhorizontal orientation, developed on a low-angle normal fault shear zone (LANF; Vojtko et al., 2018). This shear zone is related to processes of exhumation of a subvolcanic granodiorite pluton during the time span of 13.1 – 12.7 Ma (Chernyshev et al., 2013), probably accompanied by a sector collapse of the hosting stratovolcano (Kubač et al., 2018[a]). Much younger hydrothermal activity associated with rhyolite volcanism is related to the resurgent horst uplift in the centre of the caldera (12.2 – 11.4 Ma), resulted in extensive steeply-dipping system of base metal veins, cutting and displacing the earlier veins (Lexa et al., 1999; Chernyshev et al., 2013).

In some active mining sections within the eastern part of the deposit the significant enrichment of silver content in ore was determined by the mining company. This increase is probably caused by presence of telluride minerals – hessite Ag_2Te and petzite Ag_3AuTe_2, which were described in earlier works from the western part of the deposit as relatively rare mineral phases (Maťo et al., 1996; Jeleň & Háber 2000; Šály et al., 2003; Jeleň et al., 2004). During a few last years it was found out that the

Manuscript received 2019-07-08
Revised version accepted 2019-10-28

presence of Te-bearing minerals in some sections of ore-bearing veins of LANF zone in the eastern part of the deposit is higher than previously reported. The association of Au-Ag tellurides and sulphides is also extended by more mineral species. Furthermore, sulphide-rich horst-related veins have higher content of Ag-Bi minerals and no gold. This contribution is focused on relatively rare Ag-Au-Te-S mineral assemblages found in LANF veins and in flotation concentrates, and on Ag-(Cu, Sb, As, Bi)-S assemblage found in horst related veins. Their position within the studied deposit and in the evolution of mineralization is discussed.

2. GEOLOGY AND MINERALOGY OF THE DEPOSIT

The deposit is hosted by the central zone of a large middle Miocene Štiavnica stratovolcano, located in the Central Slovakia Volcanic Field on the inner side of the Carpathian arc (Fig. 1a,b). The characteristic features of the andesite stratovolcano include an extensive caldera (some 20 km in diameter), a late stage resurgent horst in the caldera centre and an extensive subvolcanic intrusive complex emplaced by underground subsidence mechanism (Konečný et al., 1995).

The Rozália mine in Hodruša-Hámre village was opened in 1951 to mine Cu-Pb-Zn ore from the late Rozália epithermal base metal vein related to resurgent horst uplift. The older, epithermal Au-Ag-Pb-Zn-Cu mineralization was discovered at the end of 1980s (Gavora, 1988) during exploration for continuation of the Cu-rich base metal veins. The LANF mineralization has been mined since 1992 in the western part of the deposit (Fig. 1c) and after depletion of the ores, mining activity was almost terminated in 2002 – 2004. However, after founding of continuation to the east (Šály et al., 2008), the eastern part of the Banská Hodruša deposit is mined with annual production of 30 – 45 kt of ore containing 450 – 500 kg of Au. Typical ore grades are 13 g/t Au, 15 g/t Ag, total base metal content (Pb, Zn, Cu) in the ore is 1–2 wt. % (Bakos et al., 2017).

The older, epithermal mineralization developed in the low-angle normal fault shear zone (LANF) occurs between the 10th and 18th levels of the Rozália mine (Fig. 1c), hosted by pre-caldera andesite, near to the flat roof of a pre-mineralization subvolcanic granodiorite pluton (Maťo et al., 1996; Koděra et al., 2005; Kubač et al., 2018[a]). The Karolína, Krištof, and Agnesa vein systems are the main ore-bearing systems, generally with the E–W and ESE–WNW orientation, and shallow to moderate dip (10 – 60°) to the south (Vojtko et al., 2018). The veins are usually 0.1 – 2 m thick and dismembered by a younger set of quartz-diorite porphyry sills and segmented by steeply-dipping mineralized strike-slip to normal faults of the resurgent horst base metal veins (described below). According the recent study of LANF mineralization (Kubač et al., 2018[a]), three types of gold/electrum were determined in the eastern part of the deposit: 1) coarse-grained gold in association with base metal sulphides (galena, sphalerite, chalcopyrite, pyrite), Au-Ag tellurides (hessite and petzite) and rare Au-Ag sulphosalts (Te-polybasite, Cu-cervelleite) crystallized in quartz or carbonates; 2) fine-grained gold in associations with galena, hessite, and petzite crystallized to carbonate pores; 3) gold in association with hessite and petzite crystallized to quartz vugs. The fineness of gold varies from 73 wt. % to 92 wt. % Au. The coarse-grained gold in association with base metals is the dominant form of gold on the deposit (Maťo et al., 1996; Kubač et al., 2018[a]). According to quantitative analyse of ground ore sample performed by QEMSCAN (Quantitative Evaluation of Minerals by Scaning electron microscopy) native gold (averages Au 85 %, Ag 15 %) and electrum (25 % < Ag < 50 %) are the main gold minerals in the sample and account for ~ 92 % of the total mass of the gold minerals. Au-Ag tellurides, including hessite and petzite account for about 8 %. A few aggregates (0.3 %) were identified as an AgAuS mineral (Chovan et al., 2016[a]).

The younger system of base metal veins was controlled by faults of the resurgent horst uplifted in the central part of the caldera. Within the studied deposit this system includes Rozália, Bakali, Amália, Martin, and Ochsenkopf veins (Fig. 1c), generally NNE–SSW inclined with the average dip of 50 – 70° (Vojtko et al., 2018). Typically, these mainly contain coarse-grained base metal sulphides and Ag minerals with no visible gold. The veins are usually up to 8 km long with vertical extent up to 1000 m, and show a general zonal arrangement, related to spatial distribution of individual mineralization stages and paragenetic associations (e.g., Koděra, 1963; Kovalenker et al., 1991; Jeleň & Háber, 2000). Authors distinguished four vertical zones with variable thickness: upper Au-Ag zone (150 – 200 m), upper Pb-Zn zone (150 – 300 m), lower Pb-Zn zone (300 – 400 m) and Cu zone (up to 500 m). Lower vertical zones of these veins (300 – 500 m) occur at the levels of the LANF mineralization, typically with base metal sulphides, and Ag minerals like Ag-tetrahedrite, acanthite, and polybasite. Other various Cu-Pb-Bi sulphosalts of cuprobismutite, pavonite, and aikinite homologous series and galena-matildite solid solutions were found in the Rozália mine deposit (Jeleň et al., 2012).

3. METHODOLOGY

Representative samples of both styles of mineralization were taken from the eastern part of the deposit during the years 2012–2018, from active mining works between 13th and 17th level of the Rozália mine and associated exploration drill holes. Samples of flotation concentrates from the ore-dressing plant were also studied. In total, 12 flotation concetrates and 1 technological sample (55 kg of grinded sample before the flotation treatment) were collected between the years 2014 – 2017. Au-Ag minerals were found in concentrates produced in April 2014 and February 2015, and in technological sample produced in October 2015. During this period, the mineralization related to shear zone (LANF) was mined on the studied deposit.

Standard polished thin sections were made and documented in reflected (RPL) and transmitted (TPL) polarized light with Leica DM2500 optical microscope. Back-scattered electron imaging and wavelength-dispersive (WDS) X-ray spectroscopy were performed with JEOL JXA-8530F and Cameca SX-100 electron probe micro-analysers (Earth Science Institute of Slovak Academy of Sciences and State Geological Institute of Dionýz Štúr,

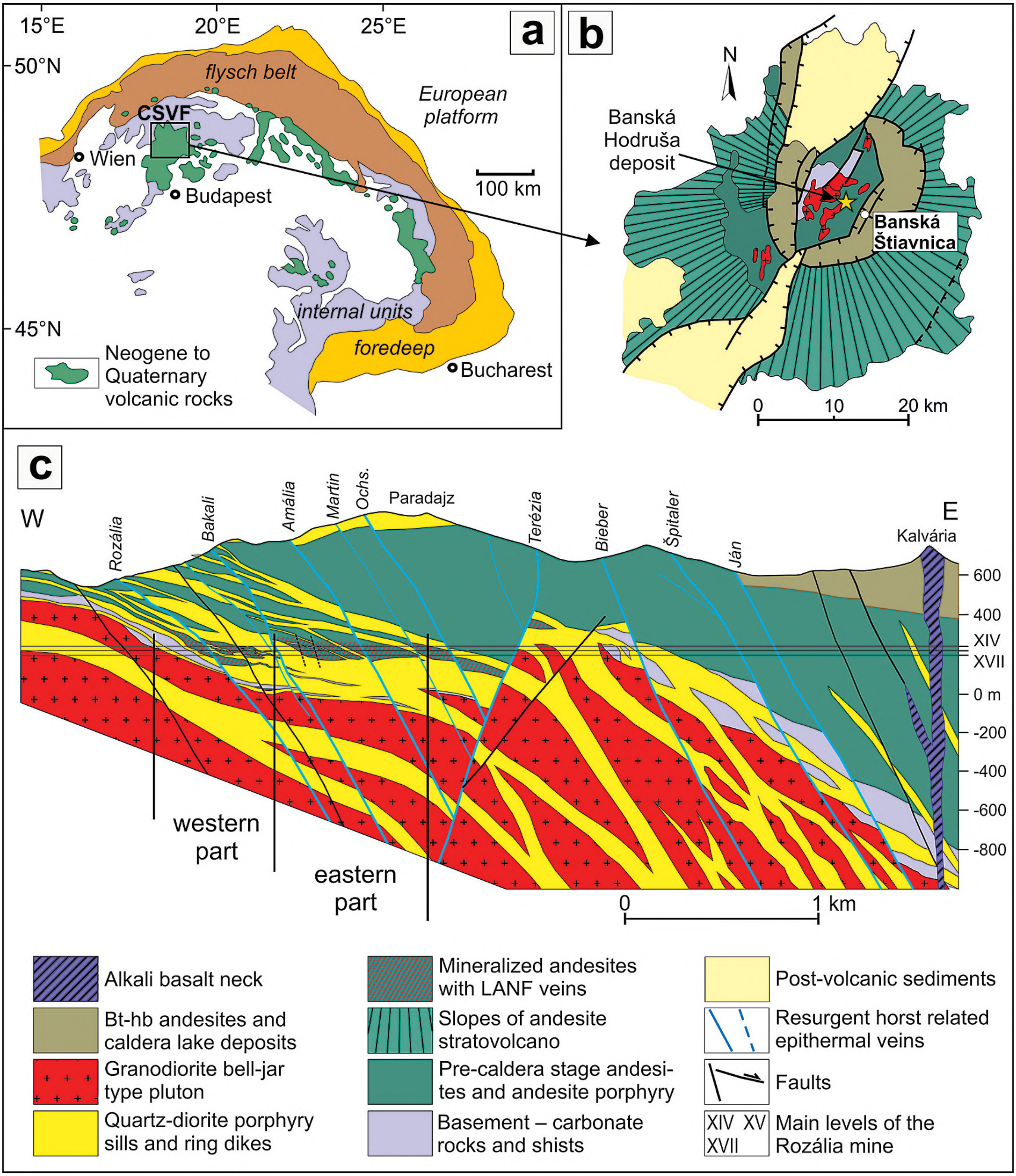

Fig. 1. Structural position and geology of the Banská Hodruša precious and base metal deposit at the Rozália Mine (Lexa et al., 1999; Kubač et al., 2018[a]). (a) Position of the Central Slovakia Volcanic Field (CSVF) within the Neogene to Quarternary volcanics of the Carpathian arc and Pannonian basin. (b) Simplified structural scheme of the Štiavnica Stratovolcano. (c) A general section of the deposit showing position of mineralized rocks with ore veins at the base of the pre-caldera andesite complex.

Slovakia). For the WDS analyses, these analytical conditions were used: native gold, tellurides, and sulphosalts-accelerating voltage 25 kV, current 15 nA, beam diameter 1 – 3 μm, ZAF correction, Ag(La) PETL – hAg, S (Ka) PETL – pyrite, Cu (Ka) LIFL – chalcopyrite, As (La) TAP – GaAs, Se (La) TAP – Bi_2Se_3, Au (Ma)PETH – Au, Te (La) PETH – CdTe, Sb (La) PETH – stibnite, Hg (Ma) PETJ –cinnabar, Bi (Ma) PETJ – bismuthine, Fe (Ka)LIFL – hematite, Pb (Ma) PETH – galena.

4. RESULTS

The following chapters described mineral phases, which forming Au-Ag-Te-S assemblage in samples of epithermal mineralization related to the low-angle normal fault shear zone (LANF), and in samples of flotation concentrates from the dressing plant. Minerals of Ag-(Bi, Cu, Sb, As)-S assemblage, which were found in samples of younger epithermal mineralization related to resurgent horst uplift (including exploration drill-core sample) are also described.

4.1. Au-Ag-Te-S assemblage in the LANF veins

Gold/electrum, hessite, petzite, Cu-cervelleite, Te-polybasite, altaite, and unnamed AgPbTeS mineral were found in Ag-rich samples from subhorizontal veins related to LANF zone. Hessite, petzite, gold/electrum, and altaite predominantly occur in association with base metal sulphides (mainly in galena), or crystalized to the free space of quartz and carbonates. Cu-cervelleite, Te-polybasite, and AgPbTeS phase are rare and were found in sulphide-rich vein in association with galena, sphalerite, chalcopyrite, hessite, and gold. Studies of mineral assemblages with gold, hessite, petzite, Te-polybasite, and Cu-cervelleite in the eastern part of the deposit have been published in summary article by Kubač et al. (2018[a]). In the following text the results of extended mineralogical study of these minerals is presented.

Hessite together with gold/electrum is the main Ag-bearing mineral on the studied deposit. It predominantly occurs in the form of anhedral grains in galena associated with petzite, gold/electrum, typically crystallized together in cavities and pores in quartz or carbonates (Fig. 2a). The intimate intergrowths of these minerals are very common. Sphalerite, chalcopyrite, and pyrite are often also present. However, intergrowths of these minerals with hessite are uncommon. In sulphide-rich Agnesa vein the Au-bearing hessite was identified in association with hessite and gold (Fig. 2b). Rarely, cervelleite, Ag-bearing galena, and unnamed AgPbTeS can occur in hessite crystals (Fig. 2c,d). In reflected polarized light hessite has grey colour (darker than galena) with greenish grey shade, reflectivity is medium and lower than galena. Anisotropy is sometimes well visible with brownish yellow and blue grey colour effects. Bireflectance is weak; however, zones with brownish and greyish shades are distinguishable. Representative EPMA analyses of hessite from LANF vein are shown in Table 1. On the basis of 3 atoms, the average of 29 analyses gives the empirical formula $(Ag_{2.00}Au_{0.01})_{2.01}Te_{0.98}$, which complies well with the theoretical formula Ag_2Te. Au-hessite is very rare and its chemical composition was determined only by two analyses (0.13 *apfu* Au av.; Tab.1), which gives average empirical formula $(Ag_{1.84}Au_{0.13})_{1.99}Te_{1.01}$. Projections of all EPMA analyses are shown on Ag-Te-Au plot diagram (Fig. 3a).

Petzite is the second most common telluride mineral on the studied deposit. It typically occurs in the form of irregular grains or aggregates in association with hessite, gold/electrum and galena (Fig. 2a). Intimate intergrowths of petzite and hessite are very common. In reflected polarized light it is distinguishable by light grey colour (darker than galena), medium reflectivity and by isotropy. Representative EPMA analyses of petzite are shown in Table 1. On the basis of 6 atoms, the average of 31 analyses gives the empirical formula $Ag_{3.08}Au_{0.95}(Te_{1.91}Se_{0.05}S_{0.01})_{1.97}$ (theoretical formula Ag_3AuTe_2). Projections of all EPMA analyses are shown on Ag-Te-Au plot diagram (Fig. 3a).

Gold/electrum with zonal texture was found in one sample (Krištof vein) where it typically occurs as large grains visible by naked eye crystallized to quartz vugs. Galena, sphalerite, hessite, and cervelleite occur as associated minerals (Fig. 2a, b). Studied grains show considerable zonality in back-scattered electron imaging (Fig. 4). The distribution maps of elements show significant Ag enrichment mostly within the marginal zones of grains, while the middle zones are characteristic by higher Au content. The zonality is diffusive and transition between different zones is fluent. Representative EPMA analyses of gold/electrum are shown in Table 2. According to 60 analyses the Ag content in zonal gold/electrum is very variable (17.8 – 45.3 wt. %; 0.3 – 0.6 *apfu*).

Te-polybasite was found in galena where typically forms anhedral grains of < 30 μm size (Fig. 2e). Rarely, intergrowths with Cu-cervelleite, hessite, and gold can be also found. In reflected polarized light it has grey colour, lower reflectivity as galena, and it is anisotropic with green blue and brownish yellow colour effects. Representative EPMA analyses are shown in Table 1. According to 10 analyses polybasite has Te content ranging from 0.5 to 1.4 *apfu* (0.9 *apfu* av.). Cu (2.1 *apfu* av.) and As (0.16 *apfu* av.) contents are decreased in comparison to theoretical composition, while Sb content is increased (1.8 *apfu* av.). Projections of all EPMA analyses are shown on triangular Ag-Te-Au and XY As vs. Sb plot diagrams (Fig. 3a,c).

Cu-cervelleite is rare mineral and was found in samples from the Agnesa vein with increased Ag content. It typically occurs in galena in the form of intergrowths with hessite, gold/electrum, rarely with Te-polybasite (Fig. 2c). Rarely, it can by also be found in hessite (Fig. 5). The size of grains does not exceed 10 μm. Cu-cervelleite was identified according to WDS analyses. Representative EPMA analyses of Cu-cervelleite are shown in Table 1. On the basis of 6 atoms, the calculated empirical formula of Cu-cervelleite (12 analyses) varies from $(Ag_{3.4}Cu_{0.15})_{3.59}Te_{0.98}S_{0.89}$ to $(Ag_{3.60}Cu_{0.31})_{3.91}Te_{1.21}S_{1.15}$. The average empirical formula of Cu-cervelleite is $(Ag_{3.82}Cu_{0.22})_{3.86}Te_{1.05}S_{1.05}$. Ideal cervelleite with empirical formula close to theoretical Ag_4TeS was not found in this mineral association. Cervelleite is significantly enriched in Cu, which ranges from 0.15 to 0.3 *apfu*. Projections of all EPMA analyses are shown on Ag-Te-Au plot diagram (Fig. 3a). The average Te/S ratio corresponds to 1.0. Occupation on cationic position (Cu+Ag) varies between 3.63 and 4.0.

Altaite is very rare mineral and was found in one sample from the Krištof vein. It occurs in form of tiny inclusions (< 6 μm) in hessite (Fig. 2f). Gold and petzite are associated minerals. Due to higher reflectivity compared to hessite it can be easily recognized in reflected polarized light. Representative EPMA analyses are shown in Table 1. On the basis of 2 atoms, the average of 3 analyses gives the empirical formula $(Pb_{0.99}Ag_{0.1})_{1.0}Te_{1.00}$.

AgPbTeS phase was found in a sample from the Agnesa vein system, where it occurs in the form of myrmekites in hessite (Figs. 2d, 5). Representative EPMA analyses are shown in Table 1. On the basis of 4 atoms, the average of 4 analyses gives

Tab. 1. Representative EPMA analyses and calculated formulae of hessite, Au-hessite, petzite, Te-polybasite, Cu-cervelleite, klausthalite, altaite, and AgPbTeS phasefrom epithermal mineralization related to shear zone (LANF).

Mineral	Au	Ag	Hg	Cu	As	Pb	Sb	Bi	Te	Se	S	Σ
						EPMA results (wt.%)						
hs	0.11	63.43	0.00	0.00	0.01	n.a.	0.00	0.00	35.96	0.00	0.03	99.53
hs	0.53	63.16	0.00	0.04	0.00	n.a.	0.00	0.00	36.06	0.00	0.05	99.84
hs	0.73	63.23	0.01	n.a.	0.00	n.a.	n.a.	0.03	36.08	0.04	0.03	100.14
hs	0.05	63.05	0.02	0.01	0.00	0.00	0.29	0.00	37.00	0.00	0.09	100.54
hs(Au)	4.89	57.34	0.10	0.00	0.00	0.10	0.29	0.06	36.52	0.00	0.16	99.49
hs(Au)	9.01	53.48	0.18	0.00	0.00	0.00	0.31	0.11	35.13	0.03	0.10	98.38
pz	24.76	42.51	0.08	0.00	0.01	n.a.	n.a.	0.00	32.22	0.00	0.02	99.58
pz	25.92	42.99	0.04	n.a.	0.00	n.a.	n.a.	0.00	30.41	0.64	0.07	100.06
pz	23.85	43.57	0.02	n.a.	0.00	n.a.	n.a.	0.01	32.36	0.60	0.00	100.42
pz	24.20	44.15	0.10	n.a.	0.00	n.a.	n.a.	0.00	31.77	0.59	0.03	100.84
pz	24.94	43.41	0.00	n.a.	0.00	n.a.	n.a.	0.00	31.97	0.67	0.03	101.02
plb	0.00	65.75	0.01	5.50	0.44	n.a.	9.29	0.00	5.13	0.00	12.68	98.81
plb	0.00	65.75	0.13	4.83	0.66	n.a.	8.44	0.04	7.18	0.00	13.16	100.20
plb	0.00	64.16	0.04	6.39	0.44	0.33	10.30	0.00	2.77	0.05	13.42	97.89
crv	0.01	68.04	0.01	1.93	0.06	0.06	0.00	0.09	23.30	0.00	4.69	98.20
crv	0.00	68.01	0.00	3.42	0.00	n.a.	0.11	0.00	22.32	0.00	6.09	99.95
crv	0.04	66.06	0.02	3.16	0.00	n.a.	0.15	0.00	22.76	0.00	6.19	98.38
crv	0.00	67.45	0.00	2.46	0.00	0.01	0.19	0.00	23.79	0.00	6.00	99.96
clh	n.a.	0.17	0.00	n.a.	0.00	76.81	0.00	0.00	n.a.	19.23	4.12	100.34
clh	n.a.	0.14	0.00	n.a.	0.00	77.31	0.00	0.00	n.a.	17.51	5.13	100.09
alt	n.a.	0.26	n.a.	0.00	n.a.	60.49	n.a.	n.a.	37.31	n.a.	n.a.	98.06
alt	n.a.	0.37	n.a.	0.00	n.a.	60.85	n.a.	n.a.	37.27	n.a.	n.a.	98.49
AgPbTeS	0.00	37.67	0.00	0.01	0.00	33.57	0.21	0.00	23.57	0.00	5.35	100.38
AgPbTeS	0.00	35.77	0.00	0.00	0.00	37.53	0.21	0.00	20.92	0.13	5.72	100.28
						Calculated formulae based on 3 (hs), 4 (AgPbTeS), 6 (pz, crv), 29 (plb) and 2 (clh, alt) apfu						
hs	0.00	2.02	0.00	0.00	0.00	-	0.00	0.00	0.97	0.00	0.00	3.00
hs	0.01	2.01	0.00	0.00	0.00	-	0.00	0.00	0.97	0.00	0.01	3.00
hs	0.01	2.01	0.00	-	0.00	-	-	0.00	0.97	0.00	0.00	3.00
hs	0.00	1.99	0.00	0.00	0.00	0.00	0.01	0.00	0.99	0.00	0.01	3.00
hs(Au)	0.09	1.87	0.00	0.00	0.00	0.00	0.01	0.00	1.01	0.00	0.02	3.00
hs(Au)	0.17	1.80	0.00	0.00	0.00	0.00	0.01	0.00	1.00	0.00	0.01	3.00
pz	0.98	3.06	0.00	0.00	0.00	-	-	0.00	1.96	0.00	0.00	6.00
pz	1.01	3.07	0.00	-	0.00	-	-	0.00	1.84	0.06	0.02	6.00
pz	0.92	3.08	0.00	-	0.00	-	-	0.00	1.93	0.06	0.00	6.00
pz	0.93	3.11	0.00	-	0.00	-	-	0.00	1.89	0.06	0.01	6.00
pz	0.96	3.06	0.00	-	0.00	-	-	0.00	1.91	0.06	0.01	6.00
plb	0.00	14.56	0.00	2.07	0.14	0.00	1.82	0.00	0.96	0.00	9.45	29.00
plb	0.00	14.35	0.02	1.79	0.21	0.00	1.63	0.00	1.32	0.00	9.67	29.00
plb	0.00	14.04	0.01	2.37	0.14	0.04	2.00	0.00	0.51	0.01	9.88	29.00
crv	0.00	3.82	0.00	0.18	0.00	0.00	0.00	0.00	1.10	0.00	0.89	6.00
crv	0.00	3.60	0.00	0.31	0.00	-	0.00	0.00	1.00	0.00	1.08	6.00
crv	0.00	3.55	0.00	0.29	0.00	-	0.01	0.00	1.03	0.00	1.12	6.00
crv	0.00	3.61	0.00	0.22	0.00	0.00	0.01	0.00	1.08	0.00	1.08	6.00
clh	-	0.00	0.00	-	0.00	1.00	0.00	0.00	-	0.65	0.35	2.00
clh	-	0.00	0.00	-	0.00	0.99	0.00	0.00	-	0.59	0.42	2.00
alt	-	0.01	-	0.00	-	1.00	-	-	1.00	-	-	2.00
alt	-	0.01	-	0.00	-	1.00	-	-	0.99	-	-	2.00
AgPbTeS	0.00	1.61	0.00	0.00	0.00	0.75	0.01	0.00	0.85	0.00	0.77	4.00
AgPbTeS	0.00	1.54	0.00	0.00	0.00	0.84	0.01	0.00	0.76	0.01	0.83	4.00

hs – hessite; hs(Au) – Au-hessite; pz – petzite; plb – Te-polybasite; crv – Cu-cervelleite; clh – clausthalite; alt – altaite; n.a. – not analyzed

the empirical formula $Ag_{1.60}Pb_{0.79}Te_{0.80}S_{0.79}$. The Pb content in AgPbTeS phase is significantly higher than in Cu-cervelleite, while the Ag content is decreased.

Clausthalite is very rare mineral on the studied deposit and was found only in one sample of the LANF vein enriched by Se and Te (Chovan et al., 2016[b]). Itis the miscibility phase between

Tab. 2. Representative EPMA analyses and calculated formulae of gold/electrum from epithermal mineralization related to shear zone (LANF).

Au	Ag	Hg	Cu	Fe	Bi	Ni	Te	S	Σ
				EPMA results (wt. %)					
55.07	45.29	0.00	0.00	0.03	0.11	0.00	0.51	0.02	101.02
57.09	44.31	0.00	0.00	0.00	0.12	0.00	0.11	0.12	101.76
58.48	42.31	0.00	0.00	0.00	0.09	0.02	0.57	0.05	101.50
59.84	40.09	0.00	0.00	0.02	0.00	0.02	0.14	0.07	100.18
62.05	38.68	0.00	0.00	0.00	0.07	0.01	0.10	0.02	100.92
64.99	35.37	0.00	0.00	0.01	0.19	0.01	0.34	0.03	100.93
68.20	32.42	0.00	0.00	0.00	0.24	0.00	0.04	0.04	100.95
73.82	28.03	0.00	0.00	0.01	0.07	0.00	0.08	0.01	102.02
79.82	20.33	0.00	0.00	0.00	0.21	0.01	0.05	0.04	100.46
81.24	19.68	0.00	0.00	0.00	0.21	0.00	0.02	0.10	101.25
83.58	17.77	0.00	0.00	0.00	0.02	0.00	0.00	0.01	101.38
				Calculated formulae based on 1 apfu					
0.40	0.60	0.00	0.00	0.00	0.00	0.00	0.01	0.00	1.00
0.41	0.58	0.00	0.00	0.00	0.00	0.00	0.00	0.01	1.00
0.43	0.56	0.00	0.00	0.00	0.00	0.00	0.01	0.00	1.00
0.45	0.55	0.00	0.00	0.00	0.00	0.00	0.00	0.00	1.00
0.47	0.53	0.00	0.00	0.00	0.00	0.00	0.00	0.00	1.00
0.50	0.49	0.00	0.00	0.00	0.00	0.00	0.00	0.00	1.00
0.53	0.46	0.00	0.00	0.00	0.00	0.00	0.00	0.00	1.00
0.59	0.41	0.00	0.00	0.00	0.00	0.00	0.00	0.00	1.00
0.68	0.32	0.00	0.00	0.00	0.00	0.00	0.00	0.00	1.00
0.69	0.30	0.00	0.00	0.00	0.00	0.00	0.00	0.00	1.00
0.72	0.28	0.00	0.00	0.00	0.00	0.00	0.00	0.00	1.00

clausthalite and galena and typically forms tiny rims (<15 μm) in galena. Due to similar optical parameters as galena its identification was based on WDS analyses. Representative EPMA analyses of clausthalite are shown in Table 1. On the basis of 2 atoms, the average of 8 analyses gives the empirical formula $Pb_{1.0}(Se_{0.6}S_{0.4})_{1.0}$. The Se content in clausthalite ranges between 0.44 and 0.66 *apfu*, while the S content between 0.34 and 0.42 *apfu*.

4.2. Au-Ag-Te-S assemblage in flotation concentrates

Calaverite, krennerite, sylvanite, unnamed AgAuTeS phase, hessite, Au-hessite, petzite, uytenbogaardtite, and petrovskaite were found in samples of flotation concentrates. They occur together and typically replace the primary gold grains. Uytenbogaardtite and petrovskaite typically form thin rims around gold or other Au-Ag minerals.

Calaverite, **krennerite,** and **sylvanite** were found rarely in the form of intergrowns with gold, hessite, petzite, uytenbogaardtite, petrovskaite, and unnamed AgAuTeS phase (Figs. 6, 7,8a). The size of grains does not exceed 15 μm. Optical recognition of these minerals in ore microscope is impossible due to similar optical parameters. They had white colour, high reflectivity and weak bireflectance. Anisotropy is barely visible due to greyish colour shades. However, aggregates of these Au-Ag tellurides can be easily recognized from other associated minerals (hessite, petzite, uytenbogaardtite, and petrovskaite) due to their reflectivity and colour (Figs. 6, 7a,c). Accurate identification of minerals is based on their chemical composition by WDS analyses and back-scattered electron imaging. Representative EPMA analyses of calaverite ($AuTe_2$), krennerite (Au_3AgTe_8), and sylvanite ($AgAuTe_4$) are shown in Table 3. The average calculated empirical formula for individual minerals are: for calaverite $(Au_{0.93}Ag_{0.09})_{1.02}(Te_{1.95}S_{0.01})_{1.96}$ (18 analyses); for krennerite $Au_{3.36}Ag_{1.09}(Te_{7.34}S_{0.15})_{7.49}$ (7 analyses); and for sylvanite $Au_{1.4}Ag_{0.91}(Te_{3.58}S_{0.07})_{4.05}$ (5 analyses). Chemical composition of calaverite is close to theoretical, only with a slight increase in Ag (0.1 *apfu* av.). Krennerite shows increase in Au (3.4 *apfu* av.) and decrease in Te (7.3 *apfu* av.), as well as sylvanite (1.4 *apfu* Au av. and 3.6 *apfu* Te av.). Projections of all EPMA analyses are shown on Ag-Te-Au plot diagram (Fig. 3b).

Hessite from flotation concentrates was found in association with gold, petzite, calaverite, krennerite, and sylvanite. Hessite or Au-bearing hessite forms tiny rims around petzite or sylvanite, or marginal zones around calaverite, krennerite, sylvanite, and petzite (Figs. 6, 8a,b). Representative EPMA analyses of hessite from flotation concentrates are shown in Table 3. On the basis of 3 atoms, the average of 15 analyses gives the empirical formula $(Ag_{1.92}Au_{0.05})_{1.97}(Te_{0.92}S_{0.1})_{1.03}$ (theoretical formula Ag_2S). Significant enrichment was determined in Au content (from 0.01 to 0.12 *apfu*) and S content (up to 0.26 *apfu*). Projections of all EPMA analyses are shown on Ag-Te-Au plot diagram (Fig. 3b).

Petzite is relatively rare in the assemblage, typically occurs in form of intergrowth aggregates with gold, hessite, galena, rarely with sylvanite, krennerite, and calaverite (Figs. 6, 8b). Representative EPMA analyses of petzite from flotation concetrates are shown in Table 3. On the basis of 6 atoms, the average of 5 analyses gives the empirical formula $Ag_{2.95}Au_{0.98}(Te_{2.01}S_{0.03})_{2.04}$, which agrees well with the theoretical formula Ag_3AuTe_2. The heterogenity of petzite (Fig. 6) is caused by variability of Au content in the individual phases (from 0.9 to 1.0 *apfu* Au).

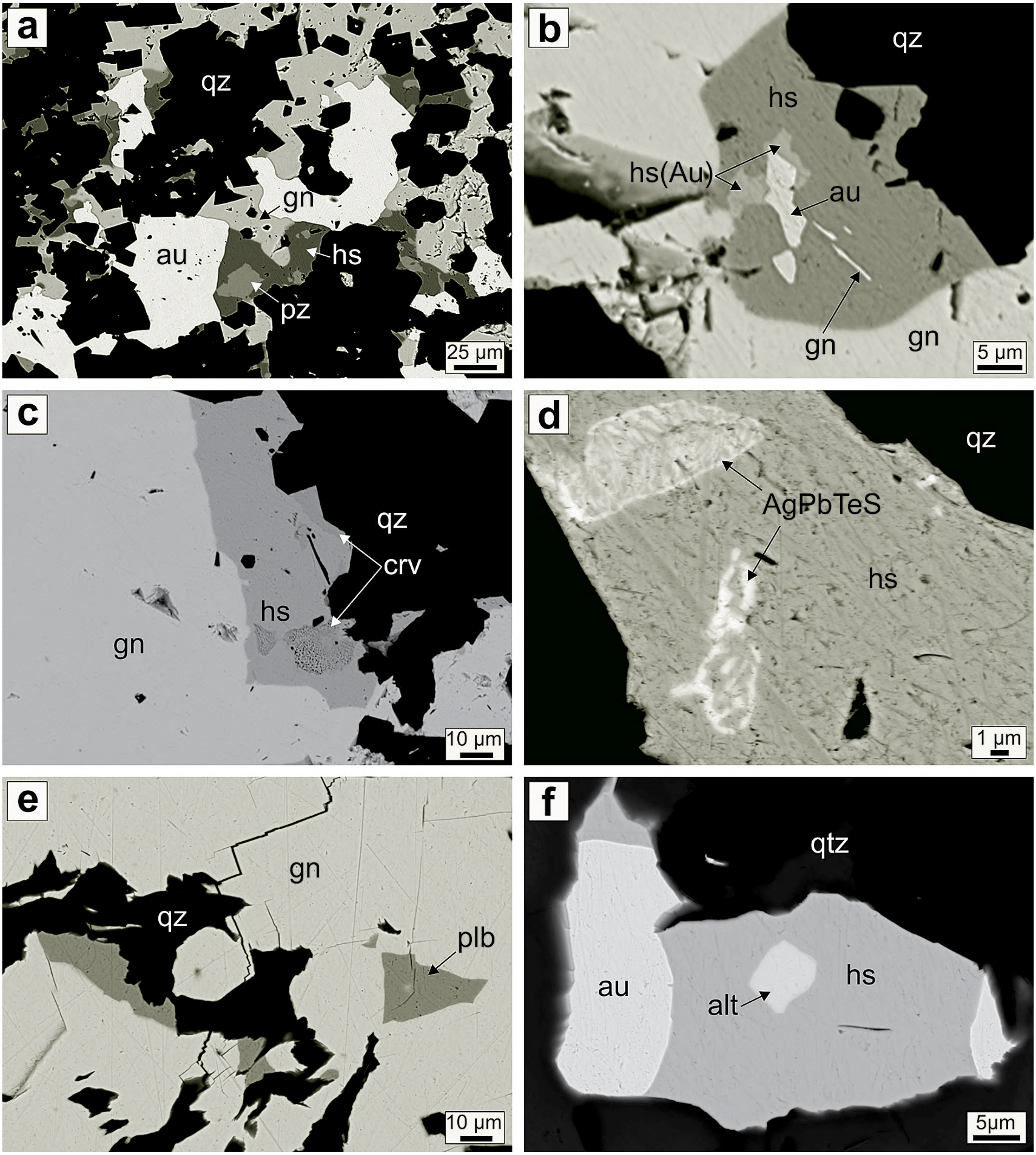

Fig. 2. Back-scattered electron images of Au-Ag-Te-S assemblage in LANF veins. (a) Intergrowth of gold, galena, petzite, and hessite in quartz. Hessite shows brownish blue colour effects of anisotrophy; (b) Intergrowth of hessite and Au-hessite around gold grain, together in galena; (c) Intergrowth of hessite and Cu-cervelleite in galena; (d) Detail of myrmekite intergrowth of AgPbTeS phase and hessite; (e) Grains of Te-polybasite in galena; (f) Inclusion of altaite crystallized in hessite. Abbreviations: alt – altaite; au – gold; crv – Cu-cervelleite; gn – galena; hs – hessite; plb – Te-polybasite; pz – petzite; qz – quartz.

Projections of all EPMA analyses are shown on Ag-Te-Au plot diagram (Fig. 3b).

AgAuTeS phase was identified as intergrowths with krennerite and hessite, or as irregular grains rimmed by uytenbogaardtite and petrovskaite. It also replaces gold together with calaverite/krennerite and uytenbogaardtite (Fig. 7a,b). Identification in ore microscope is difficult due to similar colour and reflectivity as hessite and uytenbogaardtite. Optical distinction from krennerite/sylvanite is easier due to their white colour and high reflectivity. Representative EPMA analyses of AgAuTeS mineral are shown in Table 3. On the basis of 4 atoms, the average of 6 analyses gives the empirical formula $Ag_{1.98}Au_{1.04}Te_{0.60}S_{0.36}$.

Tab. 3. Representative EPMA analyses and calculated formulae of calaverite, krennerite, sylvanite, hessite, Au-hessite, petzite, uytenbogaardtite, petrovskaite, and AgAuTeS phase from flotation concentrates.

Mineral	Au	Ag	Hg	Cu	As	Fe	Pb	Sb	Bi	Te	Se	S	Σ
EPMA results (wt.%)													
clv	45.65	1.78	n.a.	n.a.	0.00	n.a.	n.a.	n.a.	n.a.	51.61	n.a.	0.21	99.25
clv	37.87	3.37	0.46	n.a.	0.00	n.a.	n.a.	n.a.	0.45	56.29	0.00	0.02	98.45
clv	41.53	1.48	0.00	0.05	0.00	0.04	0.19	0.37	0.02	55.97	0.00	0.02	99.68
krn	35.36	5.41	0.58	n.a.	0.00	n.a.	n.a.	n.a.	0.21	56.56	0.26	0.06	98.43
krn	33.03	7.80	n.a.	n.a.	0.00	n.a.	n.a.	n.a.	n.a.	57.56	n.a.	0.06	98.45
krn	38.69	6.30	0.01	0.10	0.00	0.02	0.24	0.31	0.00	53.81	0.00	0.21	99.67
slv	30.10	14.54	0.52	n.a.	0.00	n.a.	n.a.	n.a.	0.24	52.16	0.09	0.55	98.21
slv	30.27	11.30	0.00	0.06	0.00	0.04	0.16	0.37	0.06	57.10	0.00	0.06	99.41
hs(Au)	5.60	58.63	n.a.	n.a.	0.00	n.a.	n.a.	n.a.	n.a.	34.78	n.a.	1.03	100.04
hs(Au)	6.84	59.91	n.a.	n.a.	0.00	n.a.	n.a.	n.a.	n.a.	31.52	n.a.	2.03	100.30
hs	1.16	63.63	0.00	n.a.	0.00	n.a.	n.a.	n.a.	0.13	31.40	0.00	2.19	98.51
hs	0.75	63.10	n.a.	n.a.	0.08	n.a.	n.a.	0.00	0.00	35.59	n.a.	0.15	99.67
pz	25.23	40.50	0.58	n.a.	0.00	n.a.	n.a.	n.a.	0.17	32.62	0.01	0.05	99.17
pz	23.34	41.22	0.57	n.a.	0.00	n.a.	n.a.	n.a.	0.32	33.82	0.14	0.04	99.45
uyt	33.87	50.81	0.89	0.29	0.00	n.a.	n.a.	0.00	0.04	2.52	0.19	12.36	100.97
uyt	24.49	56.04	0.59	0.25	0.00	n.a.	n.a.	0.00	0.15	4.85	0.07	13.21	99.64
ptr	55.90	31.98	n.a.	n.a.	n.a.	n.a.	0.31	n.a.	n.a.	2.24	0.04	7.61	98.08
ptr	59.76	30.32	n.a.	n.a.	n.a.	n.a.	0.57	n.a.	n.a.	1.79	0.00	5.68	98.11
AgAuTeS	41.64	43.15	0.75	n.a.	0.00	n.a.	n.a.	n.a.	0.30	12.99	0.11	2.72	101.67
AgAuTeS	35.56	45.12	0.91	n.a.	0.00	n.a.	n.a.	n.a.	0.25	17.96	0.00	1.55	101.35
AgAuTeS	38.21	41.20	0.75	n.a.	0.00	n.a.	n.a.	n.a.	0.31	15.18	0.00	4.57	100.21
Calculated formulae based on 3 (hs, clv, ptr), 4 (AgAuTeS), 6 (pz, uyt, slv) and 12 (krn) apfu													
clv	1.05	0.07	-	-	0.00	-	-	-	-	1.84	-	0.03	3.00
clv	0.86	0.14	0.01	-	0.00	-	-	-	0.01	1.98	0.00	0.00	3.00
clv	0.94	0.06	0.00	0.00	0.00	0.00	0.00	0.01	0.00	1.97	0.00	0.00	3.00
krn	3.16	0.88	0.05	-	0.00	-	-	-	0.02	7.80	0.06	0.03	12.00
krn	2.90	1.25	-	-	0.00	-	-	-	-	7.81	-	0.03	12.00
krn	3.42	1.02	0.00	0.03	0.00	0.01	0.02	0.04	0.00	7.35	0.00	0.12	12.00
slv	1.28	1.13	0.02	-	0.00	-	-	-	0.01	3.41	0.01	0.14	6.00
slv	1.29	0.88	0.00	0.01	0.00	0.01	0.01	0.03	0.00	3.76	0.00	0.02	6.00
hs(Au)	0.10	1.86	-	-	0.00	-	-	-	-	0.93	-	0.11	3.00
hs(Au)	0.12	1.85	-	-	0.00	-	-	-	-	0.82	-	0.21	3.00
hs	0.02	1.94	0.00	-	0.00	-	-	-	0.00	0.81	0.00	0.23	3.00
hs	0.01	2.01	-	-	0.00	-	-	0.00	0.00	0.96	-	0.02	3.00
pz	1.01	2.95	0.02	-	0.00	-	-	-	0.01	2.01	0.00	0.01	6.00
pz	0.92	2.97	0.02	-	0.00	-	-	-	0.01	2.06	0.01	0.01	6.00
uyt	0.97	2.67	0.03	0.03	0.00	-	-	0.00	0.00	0.11	0.01	2.18	6.00
uyt	0.68	2.83	0.02	0.02	0.00	-	-	0.00	0.00	0.21	0.00	2.24	6.00
ptr	1.02	1.06	-	-	-	-	0.01	-	-	0.06	0.00	0.85	3.00
ptr	1.17	1.08	-	-	-	-	0.01	-	-	0.05	0.00	0.68	3.00
AgAuTeS	1.05	1.99	0.02	-	0.00	-	-	-	0.01	0.51	0.01	0.42	4.00
AgAuTeS	0.91	2.11	0.02	-	0.00	-	-	-	0.01	0.71	0.00	0.24	4.00
AgAuTeS	0.92	1.81	0.02	-	0.00	-	-	-	0.01	0.56	0.00	0.68	4.00

clv – calaverite; krn – krennerite; slv – sylvanite; hs(Au) – Au-hessite; hs – hessite; pz – petzite; uyt – uytenbogaardtite; ptr – petrovskaite; n.a. – not analyzed

Projections of all EPMA analyses are shown on Ag-Te-Au plot diagram (Fig. 3b).

Uytenbogaardtite typically form very thin rims (< 3 μm) around gold/electrum and around aggregates of Au-Ag tellurides (hessite, petzite, krennerite, and sylvanite), which partially replace gold (Figs. 6, 7b). In reflected polarized light it has grey colour with brownish shade, lower reflectivity than associated minerals and it is anisotropic. Representative EPMA analyses of uytenbogaardtite are shown in Table 3. On the basis of 6 atoms, the average of 4 analyses gives the empirical formula $Ag_{2.7}Au_{0.85}(S_{2.26}Te_{0.15})_{2.41}$ (theoretical formula Ag_3AuS_2). Uytenbogaardtite has a significant enrichment in S (2.3 *apfu* av.) and Te (0.15 *apfu* av.) and depletion in Ag (2.7 *apfu* av.) and Au (0.85 *apfu* av.). Projections of all EPMA analyses are shown on Ag-Te-Au plot diagram (Fig. 3b).

Petrovskaite occurrence is very similar to uytenbogaardtite, forming thin rims around gold/electrum or around aggregates of Au-Ag tellurides (Figs. 7c,d). Representative EPMA analyses of petrovskaite are shown in Table 3. On the basis of 3 atoms, the average of 5 analyses gives the empirical formula

$Ag_{1.05}Au_{1.16}(S_{0.73}Te_{0.05})_{0.78}$. Petrovskaite has a significant enrichment in Te (0.05 *apfu* av.) in comparison with theoretical formula (AgAuS). Values of the main elements are slightly decreased (S 0.7 *apfu* av.; Ag 1.05 *apfu* av.) except for Au which is increased (1.15 *apfu* av.). Projections of all EPMA analyses are shown on Ag-Te-Au plot diagram (Fig. 3b).

4.3. Ag-(Bi, Cu, Sb, As)-S assemblage in horst-related veins

Polybasite-pearceite, acanthite, matildite, schapbachite, arcubisite, and cervelleite were found in one sample from late horst-related Amália vein, where these minerals form inclusions in base metal sulphides, predominantly in galena and form characteristic myrmekite texture. In the drill-hole sample BHS-247/8 the polybasite-pearceite and jalpaite were found. Rare tetrahedrite-tennantite was found in horst-related Rozália vein.

Polybasite-Pearceite was found in drill-core sample BHS-247/8 and also in sample taken from the mine stopes from the Amália vein. It typically occurs as grains (~ 60 μm) in galena in assemblage with matildite, cervelleite, schapbachite, and jalpaite (Figs. 9, 10a-c), together form characteristic myrmekite texture. Sphalerite, chalcopyrite, pyrite, hematite, and carbonate are associated minerals. It has grey colour and lower reflectivity than galena in reflected polarized light. Anisotropy is strong with dark blue and brownish green colour effects. Representative EPMA analyses of polybasite and pearceite are shown in Table 4. Projections of all analyses are shown on As vs. Sb plot diagram (Fig. 3c). According to 8 EPMA analyses the Sb content in polybasite varies between 1.3 and 1.8 *apfu* (1.5 *apfu* av.), and the As content between 0.03 and 0.55 *apfu* (0.3 *apfu* av.). The Cu content is generally lower in comparison to theoretical, varying between 1.0 and 3.55 *apfu* (2.46 *apfu* av.). The Bi content was increased only in three analyses (up to 0.25 *apfu*). In comparison (14 analyses), the values of As and Sb contents in pearceite ranging between 0.8 – 1.95 *apfu* As (1.37 *apfu* As av.) and 0 – 0.98 *apfu* Sb (0.5 *apfu* Sb av.). The Cu content is very close to theoretical composition in most of analyses, ranging between 1.85 and 3.9 *apfu* (3.0 *apfu* av.). The values of Ag content are higher, varying

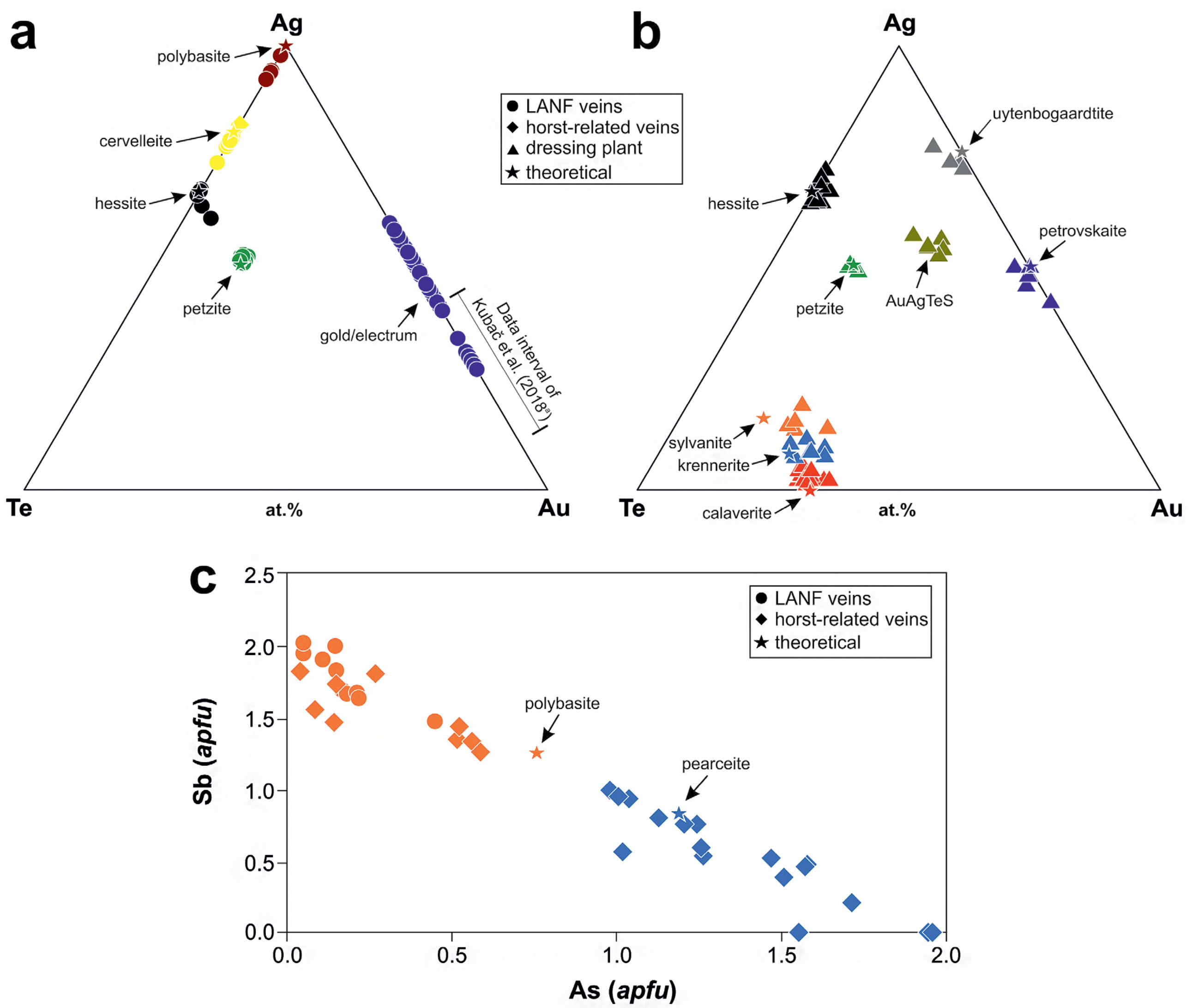

Fig. 3. A triangular Ag-Te-Au (a, b) andAs vs. Sb (c) plotdiagrams illustrating composition of Au-Ag minerals in samples of LANF veins, flotation concentrates (dressing plant) and horst-related veins from Banská Hodruša deposit. For comparison, the interval of gold analyses collected from LANF veins in eastern part of the deposit by Kubač et al. (2018a) is also shown. All data from EPMA analyses.

between 11.9 and 14.7 *apfu* (13.0 *apfu* av.). The various contents of As and Sb of polybasite and pearceite are also manifested in back-scattered electron imaging by presence of dark (As-rich) and light (Sb-rich) zones (Fig. 10b).

Acanthite typically forms tiny inclusions or irregular-shaped grains (< 40 μm) as a part of myrmekite aggregates with galena, where occurs in association with matildite, polybasite-pearceite, arcubisite, cervelleite, and other undefined AgPbBiS mineral phases (Figs. 9, 10d, e). In reflected polarized light it has grey colour and lower reflectivity than galena. Bireflectance and anisotropy was not observed. On the basis of 3 atoms, the average of 4 analyses gives the empirical formula $Ag_{1.93}(S_{1.01}Se_{0.03}Te_{0.01})_{1.05}$, which agrees well with the theoretical formula Ag_2S. Chemical composition of acanthite (Tab. 4) in comparison with theoretical composition shows decreased content of Ag (1.9 *apfu* av.) and slight increase in Se (0.03 *apfu* av.) and Te (0.01 *apfu* av.).

Matildite was identified in one sample as the main Ag-Bi bearing mineral within myrmekite aggregates with galena (Figs. 9, 10a). It predominantly occurs in form of thin tabular-shaped crystals (< 10 μm) in galena. Identification of matildite in ore microscope is difficult due to small size of grains and similar optical properties as galena. Anisotropy was observed only within the larger grains.Representative EPMA analyses of matildite are shown in Table 4. Projections of all EPMA

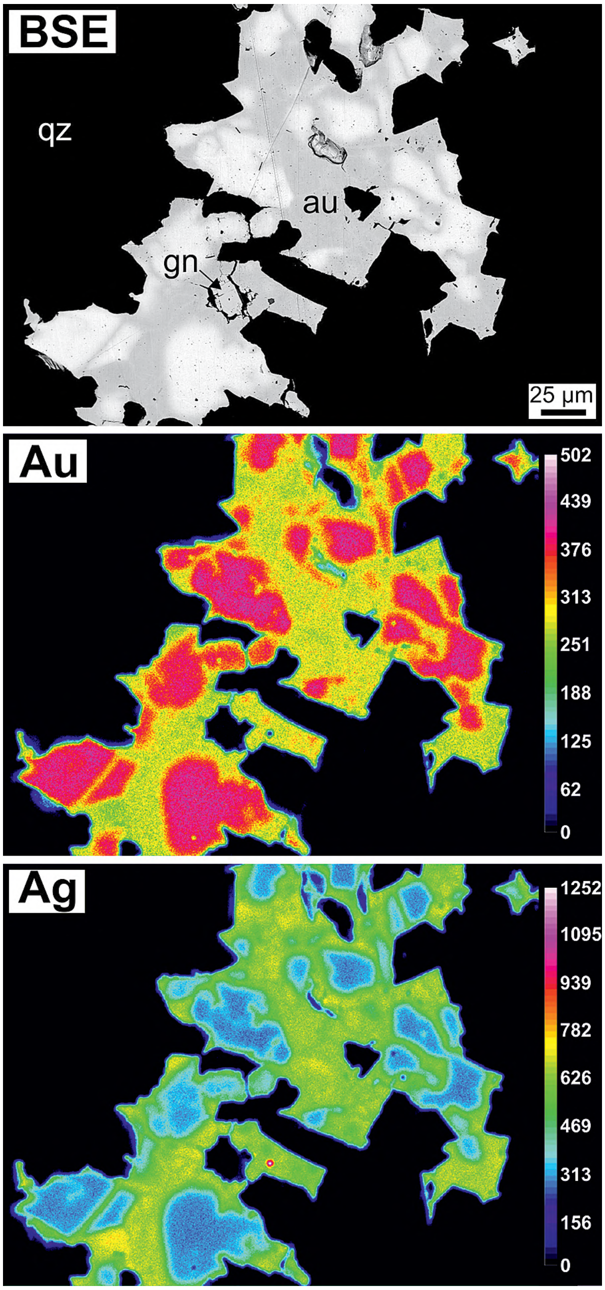

Fig. 4. Distribution of the elements (Au, Ag) in zonal gold/electrum. Note that Au content is dominant in the marginal zones, while the middle zones are Ag-rich. LANF vein. Abbreviations: au – gold; gn – galena; qz – quartz.

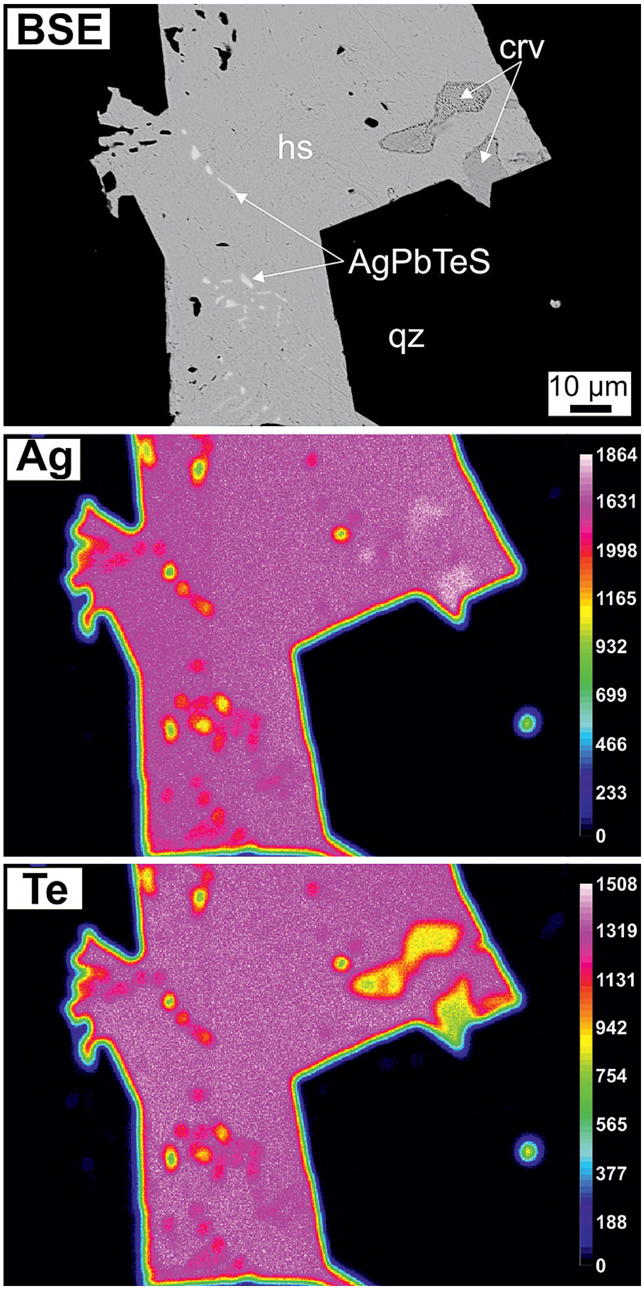

Fig. 5. Distribution map of the elements (Ag, Te) of hessite crystal with Cu-cervelleite and unnamed AgPbTeS phase. LANF vein. Abbreviations: crv – Cu-cervelleite; hs – hessite; qz – quartz.

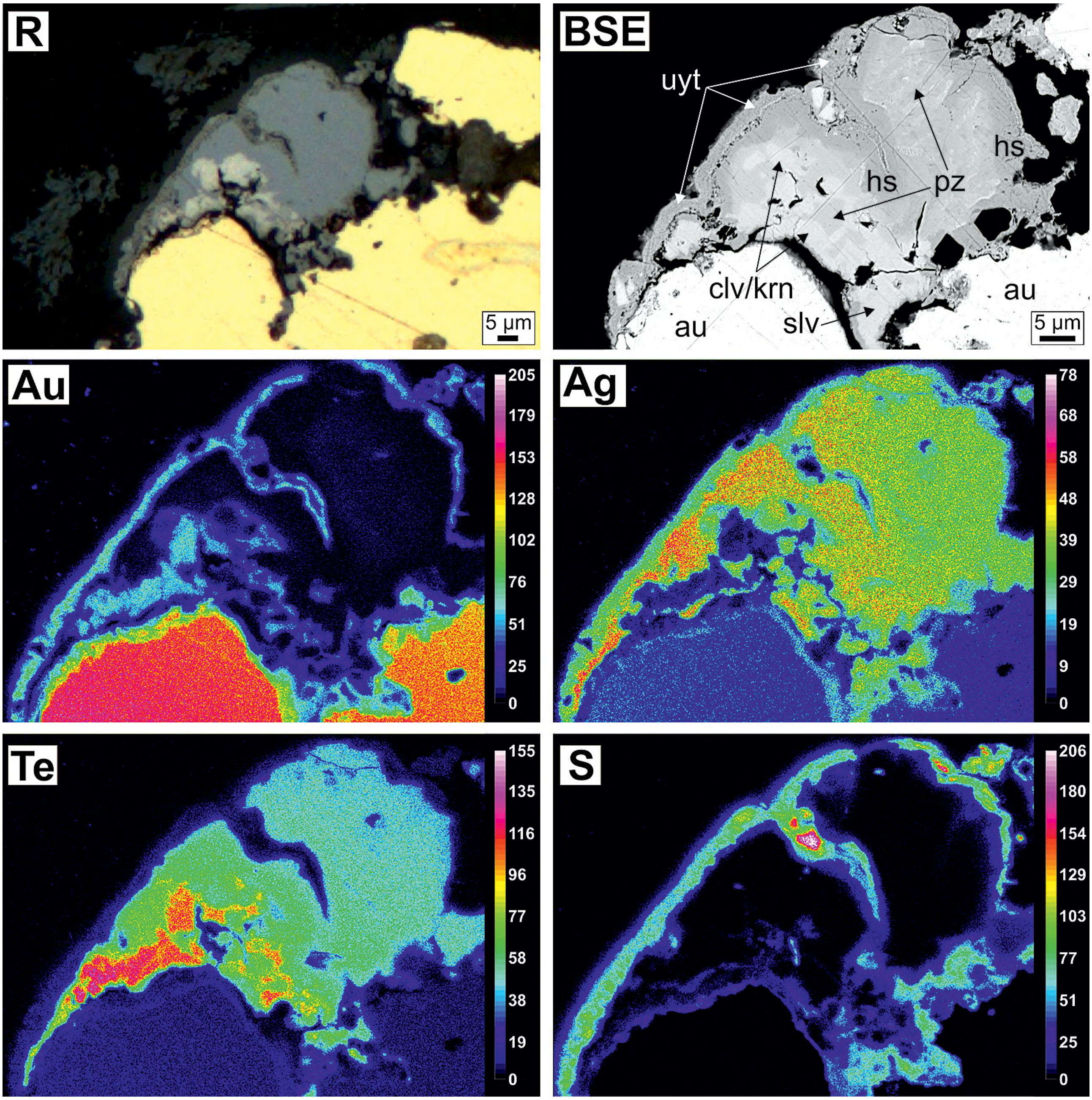

Fig. 6. Photomicrograph (reflected light) and back-scattered image showing intergrowth of hessite, petzite, calaverite/krennerite and sylvanite, together replace gold grain. Tellurides are rimmed by thin zone of uytenbogaardtite. Chemical composition of minerals is documented by distribution maps of the elements (Au, Ag, Te, S). Abbreviations: au – gold; clv – calaverite; hs – hessite; krn – krennerite; pz – petzite; slv – sylvanite; uyt – uytenbogaardtite.

analyses are shown on Bi-Ag-Pb plot diagram (Fig. 11a). On the basis of 4 atoms, the average of 3 analyses gives the empirical formula $Ag_{0.94}(Bi_{0.99}Pb_{0.07})_{1.06}(S_{1.97}Se_{0.02})_{1.99}$, which agrees well with the theoretical formula $AgBiS_2$. Matildite has significantly increased Pb content (0.07 *apfu* av.), probably caused by association with galena. A slight increase in Se was also detected (0.02*apfu* av.). Mineral composition of myrmekite textures is shown on distribution maps of elements (Fig. 9). Grey coloured crystals are characteristic by increased Ag and Bi content, which corresponds well to matildite. Very tiny needle-like inclusions could be unknown phases enriched by Bi and Ag. Needle-shaped crystals of pearceite/polybasite (or arcubiste) are characteristic by the enrichment in Ag and Cu content (without Bi). The strong Ag-enrichment is documented by the presence of acanthite.

Schapbachite was found within myrmekite aggregates of galena and Ag-Bi-Cu sulphosalts. Schapbachite grains (< 10 µm) are common in association with polybasite-pearceite and cervelleite, occurring together at the edge of galena (Fig. 10b). Optical identification in ore microscope was not possible due to its similar colour and reflectivity of galena. On the basis of 2 atoms, the one analyse gives the empirical formula $Ag_{0.43}Pb_{0.18}Bi_{0.39}S_{0.98}$, which agrees well with the theoretical formula $Ag_{0.4}Pb_{0.2}Bi_{0.4}S$. As shown in Table 4, only a slight increase was detected in Se

Tab. 4. Representative EPMA analyses and calculated formulae of polybasite, pearceite, cervelleite, acanthite, matildite, arcubisite, schapbachite, and jalpaitefrom epithermal mineralization related to horst uplift.

Mineral	Ag	Hg	Cu	As	Fe	Pb	Sb	Bi	Te	Se	S	Σ
EPMA results (wt.%)												
plb	64.31	0.00	9.28	1.78	0.29	0.08	8.05	0.00	0.00	0.00	15.95	99.72
plb	67.69	0.00	2.80	0.45	0.03	0.12	9.00	2.26	0.43	0.24	15.18	98.19
plb	63.81	0.02	10.02	1.76	0.21	0.05	7.50	0.02	0.05	0.02	16.05	99.50
prc	63.55	0.00	10.49	4.41	0.32	0.12	3.04	0.09	n.a.	n.a.	16.51	98.53
prc	63.22	0.00	10.33	3.52	0.15	0.15	5.41	0.00	n.a.	n.a.	16.61	99.39
prc	62.09	0.07	11.49	4.28	0.50	0.07	4.37	0.05	0.04	0.00	16.75	99.71
crv	72.58	0.06	0.18	0.09	n.a.	0.41	0.05	0.03	18.66	1.37	5.73	99.16
ac	86.09	0.00	0.09	0.00	0.01	0.25	0.00	0.00	0.36	0.85	13.02	100.67
ac	84.24	0.00	0.83	0.01	0.52	0.42	0.00	0.00	1.05	1.49	12.96	101.52
mtd	27.04	0.00	0.00	0.00	0.09	0.17	0.00	56.28	0.24	0.27	16.69	100.78
mtd	26.01	0.00	0.00	0.03	0.00	5.50	0.00	52.97	0.00	0.40	16.24	101.15
arc	66.14	0.00	4.18	0.70	0.01	0.06	4.62	6.87	1.59	0.74	13.31	98.22
arc	63.47	0.00	1.01	0.04	0.00	0.15	0.04	15.87	8.48	0.42	10.86	100.32
arc	60.91	0.00	3.50	0.00	0.00	0.26	0.00	16.84	5.41	1.40	11.79	100.11
scb	23.55	0.00	0.31	0.00	0.00	18.72	0.05	42.27	0.19	0.47	16.13	101.68
jlp	71.94	0.01	14.27	0.00	0.45	0.14	0.00	0.00	n.a.	n.a.	14.26	101.08
jlp	70.89	0.00	14.60	0.05	0.33	0.07	0.00	0.00	0.85	0.00	14.87	101.66
jlp	68.92	0.01	14.82	0.01	0.73	0.03	0.00	0.00	0.81	0.00	14.68	100.01
Calculated formulae based on 29 (plb, prc), 6 (crv, jlp), 3 (ac), 4 (mtd), 12 (arc) and 2 (scb) apfu												
plb	12.95	0.00	3.17	0.52	0.11	0.01	1.44	0.00	0.00	0.00	10.80	29.00
plb	14.64	0.00	1.03	0.14	0.01	0.01	1.72	0.25	0.08	0.07	11.04	29.00
plb	12.80	0.00	3.41	0.51	0.08	0.01	1.33	0.00	0.01	0.00	10.84	29.00
prc	12.57	0.00	3.52	1.26	0.12	0.01	0.53	0.00	-	-	10.98	29.00
prc	12.48	0.00	3.46	1.00	0.06	0.02	0.95	0.00	-	-	11.03	29.00
prc	12.08	0.01	3.79	1.20	0.19	0.01	0.75	0.00	0.01	0.00	10.96	29.00
crv	3.95	0.00	0.02	0.01	-	0.01	0.00	0.00	0.86	0.10	1.05	6.00
ac	1.96	0.00	0.00	0.00	0.00	0.00	0.00	0.00	0.01	0.03	1.00	3.00
ac	1.89	0.00	0.03	0.00	0.02	0.00	0.00	0.00	0.02	0.05	0.98	3.00
mtd	0.96	0.00	0.00	0.00	0.01	0.00	0.00	1.03	0.01	0.01	1.99	4.00
mtd	0.93	0.00	0.00	0.00	0.00	0.10	0.00	0.98	0.00	0.02	1.96	4.00
arc	6.15	0.00	0.66	0.09	0.00	0.00	0.38	0.33	0.12	0.09	4.16	12.00
arc	6.47	0.00	0.17	0.01	0.00	0.01	0.00	0.83	0.73	0.06	3.72	12.00
arc	6.00	0.00	0.59	0.00	0.00	0.01	0.00	0.86	0.45	0.19	3.91	12.00
scb	0.43	0.00	0.01	0.00	0.00	0.18	0.00	0.39	0.00	0.01	0.98	2.00
jlp	2.97	0.00	1.00	0.00	0.04	0.00	0.00	0.00	-	-	1.98	6.00
jlp	2.89	0.00	1.01	0.00	0.03	0.00	0.00	0.00	0.03	0.00	2.04	6.00
jlp	2.84	0.00	1.04	0.00	0.06	0.00	0.00	0.00	0.03	0.00	2.03	6.00

plb – polybasite; prc – pearceite; crv – cervelleite; ac – acanthite; mtd – matildite; arc – arcubisite; scb – schapbachite; jlp – jalpaite; n.a. – not analyzed

(0.01 *apfu*) and Cu (0.01 *apfu*). Projections of one EPMA analyse is shown on Bi-Ag-Pb plot diagram (Fig. 11a).

Arcubisite was found in one sample of horst-related Amália vein and its identification is questionable. As a part of myrmekite aggregates of galena and Ag-Bi-Cu sulphides and sulphosalts, arcubisite typically forms needle-shaped crystals intergrown with acanthite and cervelleite (Fig. 10d). Size of crystals do not exceed 60 μm. In reflected polarized light it has grey colour with greenish shade, reflectivity lower as galena, and weak anisotropy. On the basis of 12 atoms, the average of 9 analyses gives the empirical formula $Ag_{6.20}Cu_{0.41}(Bi_{0.63}Sb_{0.19})_{0.82}(S_{3.98}Te_{0.42}Se_{0.11})_{4.51}$.In comparison to theoretical formula Ag_6CuBiS_4, average chemical composition of arcubisite is quite variable (Tab. 4; Fig. 11a), with increased Ag (6.2 *apfu* av.), Te (0.4 *apfu* av.) and Sb (0.2 *apfu* av.). Bi content is slightly higher as theoretical (0.6 *apfu* av.), as well as Cu (0.4 *apfu* av.).

Cervelleite was found in horst-related Amália vein, where is a part of myrmekite aggregates of galena and Ag-Bi-Cu sulphides and sulphosalts. Primary it occurs in galena together with acanthite, arcubisite, polybasite-pearceite, and schapbachite (Fig. 10b,d,e). Cervelleite is the major Te-bearing mineral in this mineral paragenesis, although arcubisite and acanthite also contain tellurium. The grain size of cervelleite does not exceed 5 μm. In reflected polarized light it has light grey colour, reflectivity similar to galena, respectively higher than arcubisite and acanthite. On the basis of 6 atoms, the one analysis gives the empirical formula $(Ag_{3.95}Cu_{0.02})_{3.97}Te_{0.86}(S_{1.05}Se_{0.10})_{1.15}$ (Tab. 4). Silver content in cervelleite agrees well with the theoretical formula Ag_4TeS, Cu content is slightly higher (0.02 *apfu*). Significant enrichment in Se (0.1 *apfu*) corresponds to 0.1 *apfu*, while Te content has lower values than theoretical formula (Fig. 3a). (Te+Se)/S ratio corresponds to 0.92.

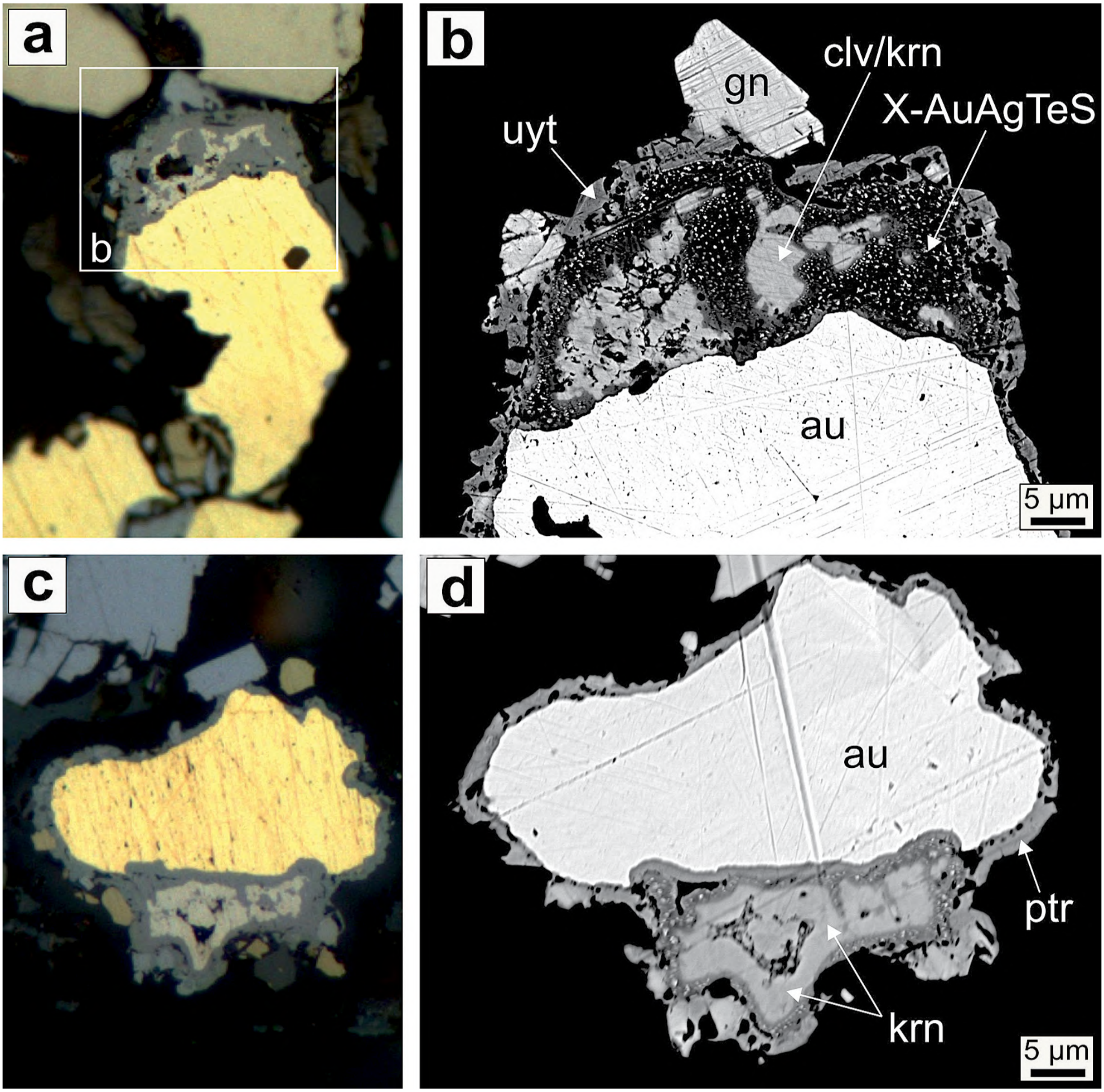

Fig. 7. Photomicrographs (reflected light) and back-scattered electron images of Au-Ag-Te-S assemblage in flotation concentrates. (a) Gold grain is replaced by Au-Ag tellurides; (b) BSE image of Fig. 7a showing aggregate of calaverite/krennerite and AgAuTeS phase, rimmed by uytenbogaardtite. AgAuTeS phase was reactable during measurement (white spots); (c) Gold grain rimmed by petrovskaite and krennerite; (d) BSE image of Fig. 7c showing tiny rim of AgAuTeS phase between krennerite and petrovskaite. Abbreviations: au – gold; clv – calaverite; gn – galena; krn – krennerite; ptr – petrovskaite; uyt – uytenbogaardtite.

Jalpaite was found in drill-core sample BHS-247/8 and is typically very rare mineral in the studied deposit. It typically forms irregular aggregates (< 60 µm) in association with polybasite-pearceite, hematite, and carbonate, together occupying interstitial areas between galena, sphalerite, and chalcopyrite (Fig. 10c). In reflected polarized light it has grey colour, low reflectivity and is very similar to polybasite-pearceite. On the basis of 6 atoms, the average of 4 analyses gives the empirical formula $Ag_{2.91}(Cu_{1.01}Fe_{0.04})_{1.05}(S_{2.02}Te_{0.03})_{2.05}$, which agrees well with the theoretical formula Ag_3CuS_2. Only slight increase in Te (0.03 *apfu* av.) and Fe (0.04 *apfu* av.) was detected (Tab. 4). Projections of all EPMA analyses are shown Bi-Ag-Pb plot diagram (Fig. 11a).

Tetrahedrite-Tennantite is rare and was found in horst-related Rozália vein sampled on 14th level in the area between the western and eastern part of the deposit (Fig. 1c). It typically occurs in form of zonal aggregates in association with base metal sulphides (sphalerite, chalcopyrite, galena, pyrite), hematite or Mn-Ca carbonates (Fig. 10f). Representative EPMA analyses of tetrahedrite and tennantite are shown in Table 5. Projections of all analyses are shown on Sb vs. As plot diagram (Fig. 11b). The average calculated empirical formula

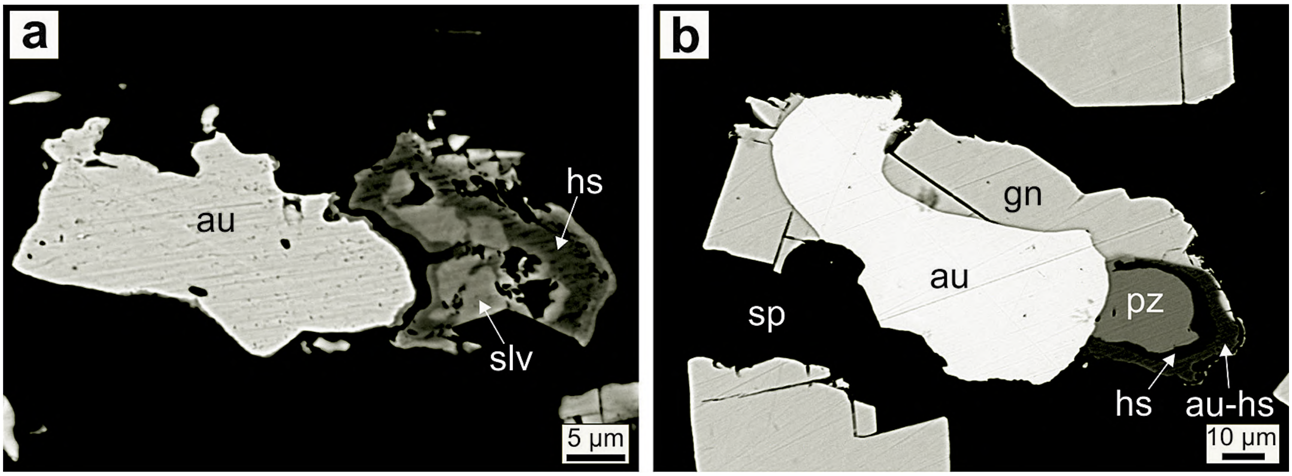

Fig. 8. Back-scattered electron images of Au-Ag-Te-S assemblage in flotation concentrates. (a) Intergrowth of gold, galena, hessite, Au-hessite, and petzite, together in sphalerite. Hessite and Au-hessite occur as tiny rims around petzite; (b) Intergrowth of gold, hessite and sylvanite. Abbreviations: au – gold; gn – galena; hs – hessite; pz – petzite; sp – sphalerite.

for individual minerals are: for tetrahedrite$(Cu_{5.78}Ag_{0.22})_{6.00}$ $[Cu_{4.05}(Zn_{1.81}Fe_{0.23}Cd_{0.15}Hg_{0.04})_{2.23}]$ $(Sb_{3.2}As_{0.77})_{3.97}S_{12.72}$ (3 analyses); and for tennantite $(Cu_{5.93}Ag_{0.07})_{6.00}[Cu_{4.33}(Zn_{1.09}Fe_{0.71}Pb_{0.03})_{1.84}]$ $(As_{3.18}Sb_{0.87})_{4.05}S_{12.77}$ (2 analyses). The oscilating zonality of tetrahedrite/tennantite aggregates represents transition from the darker tennantite (3.2 *apfu* As av.) to the lighter tetrahedrite (3.2 *apfu* Sb av.). EPMA analyses of tetrahedrite show increasing in Ag content (0.2 *apfu* av.). The Fe content is generally lower (0.23 *apfu* av.), while the Zn values are higher (1.8 *apfu* av.) in comparison to theoretical composition. Tennantite shows decreasing in Cu content (10.3 *apfu* av.) and increasing in Zn (1.1 *apfu* av.).

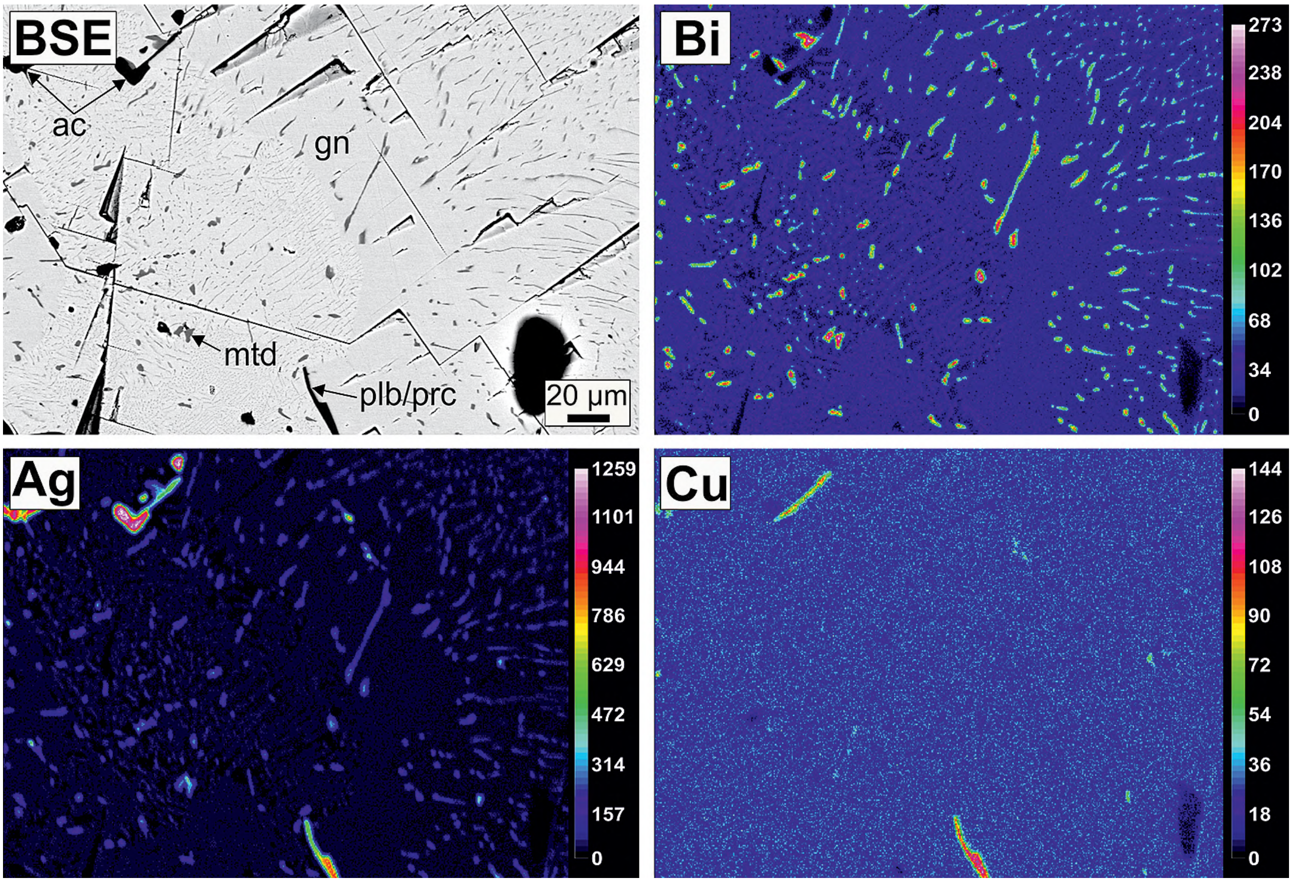

Fig. 9. Distribution map of the elements (Bi, Ag, Cu) of myrmekite texture of acanthite, matildite and polybasite/pearceite in galena. Horst-related vein. Abbreviations: ac – acanthite; gn – galena; mtd – matildite; plb/prc – polybasite/pearceite.

Tab. 5. Representative EPMA analyses and calculated formulae of tetrahedrite and tennantite + from epithermal mineralization related to horst uplift.

Mineral	Ag	Hg	Cu	Cd	As	Fe	Mn	Pb	Sb	Zn	S	Σ
EPMA results (wt. %)												
ttd	1.14	0.08	38.03	0.41	2.82	0.95	0.04	0.04	24.65	8.04	25.01	101.20
ttd	2.11	1.01	36.90	2.06	4.34	0.89	0.05	0.06	22.25	5.75	24.24	99.66
tnt	0.31	0.10	42.55	0.00	15.49	2.14	0.02	0.43	7.48	4.87	26.52	99.90
tnt	0.67	0.01	42.41	0.01	15.60	3.06	0.02	0.50	6.30	4.42	26.87	99.86
Calculated formulae based on 29 apfu												
ttd	0.17	0.01	9.78	0.06	0.61	0.28	0.01	0.00	3.31	2.01	12.75	29.00
ttd	0.33	0.08	9.76	0.31	0.97	0.27	0.01	0.01	3.07	1.48	12.71	29.00
tnt	0.04	0.01	10.31	0.00	3.18	0.59	0.01	0.03	0.95	1.15	12.73	29.00
tnt	0.09	0.00	10.20	0.00	3.18	0.84	0.01	0.04	0.79	1.03	12.81	29.00

ttd – tetrahedrite; tnt – tennantite

5. DISCUSSION

The mineralization related to low-angle normal fault shear zone (LANF) that is actually mined in the Banská Hodruša epithermal deposit has a high Au content in tens to thousands of ppm. The Ag/Au ratio in the ore is close to 1/1 (sometimes up to 10/1), the Te content is high (also sometimes Se). Described coexisting phases, which form mineral paragenetic associations (assemblages) are shown in ternary Au-Ag-Te diagram (Fig. 3a). The Au-Ag-Te-S assemblage including gold/electrum, hessite, and petzite was found in most of the samples from LANF zone in the studied part of the deposit. The presence of rare assemblage with hessite, petzite, altaite, Te-polybasite, Cu-cervelleite, gold, Ag-bearing galena, and unnamed AgPbTeS phase was also found in this type of veins. In samples of flotation concentrates the mineral assemblage with calaverite-krennerite-sylvanite, unnamed AgAuTeS phase, petzite, Au-hessite uytenbogaardtite, and petrovskaite was found (Fig. 3b). These minerals typically replace primary gold grains.

The most significant Ag-bearing mineral is telluride hessite and its occurrence together with petzite in precious-base metal veins is common. Both this minerals typically intergrow with gold and galena, and according to their growth margins they crystallize together with these minerals (Fig. 2a). The hessite-petzite intergrowth formed at temperatures below 250°C (Afifi et al., 1988[b]; Xu et al., 2012). According to Xu et al. (2012) the high-temperature cubic hessite transforms to monoclinic at temperature about 145°C, and low-temperature modification of petzite is stable at temperatures below 210°C. Cabri (1965) suggested that low hessite and low petzite were formed by breakdown of high-temperature x-phase ($Ag_{3+x}Au_{1-x}Te_2$ with $0.1 < x < 0.55$) at temperatures below 120°C. The variations of cubic and monoclinic hessite were identified by ore microscopy and their presence suggests changes in temperature and fugacity fTe_2. In some quartz veins, the presence of hessite, Au-hessite, Te-polybasite, Ag-sulphotelluride Cu-cervelleite, gold, unnamed AgPbTeS phase, and Ag-galena was found together with galena and other common sulphides (Figs. 2,5). Minerals of the Ag-Cu-Te-S system including Ag-galena, Te-polybasite, and Cu-cervelleite may be formed from the breakdown of a higher temperature galena phase (stable under 300°C) during cooling below 200°C. The indicator of crystallization may be cervelleite, formed if temperature decreases below 200°C and fugacity fTe_2 decreases compared to the values for hessite crystallization (Voudouris et al., 2011). The increasing of Cu and decreasing of Ag content in cervelleite was determined on various deposits in Romania (e.g., Băiţa Bihor, Larga, Ocna de Fier) and is caused by Cu-for-Ag substitution (Cook & Ciobanu, 2003).

The epithermal mineralization related to LANF zone crystallized from fluids of low salinity (0–4 wt. % NaCl eq.) and moderate temperatures (250–330°C) that have experienced an extensive boiling (Koděra et al., 2005; Kubač et al., 2018[b]). However, Koděra et al. (2005) interpreted rare lower homogenization temperatures (~180°C), that may represent an overprint of some late stage. Thus, this stage may correspond to mineral Au-Ag-Te-S assemblages identified in this study, which were earlier described in the western part of the deposit by Maťo et al. (1996).

Pietruszka (2016) reported the presence of cervelleite-like mineral in association with pearceite, tetrahedrite, galena, and enargite-like mineral phase in the eastern part of the deposit. The presence of Te-polybasite, tetrahedrite, and altaite was determined previously by Maťo et al. (1996) in the western part. The zonal gold/electrum (Fig. 4) is very rare within the veins of the shear zone (LANF) and was determined within the Krištof vein in association with hessite and cervelleite. Zonality and high increasing in Ag content (45.3 wt. %; 0.6 *apfu*) within the gold grains has not been determined yet in the Banská Hodruša deposit by previous studies of Maťo et al. (1996), Jeleň & Háber (2000), Števko et al. (2015) and Kubač et al. (2018[a]). However, according to Kubač et al. (2018[a]) the presence of electrum is typical for Krištof vein system, which represents the late stage of studied mineralization in the eastern part of the deposit. The systematic variation in Au/Ag content is probably related to fluid temperature changes during boiling (Hough et al., 2009). Relatively high activity of silver and decreased values of fTe_2 in the final phase of precipitation of ore minerals is demonstrated by lower Ag content in gold in association with low hessite (Afifi et al., 1988[a]; Xu et al., 2012). Selenide mineral clausthalite in association with galena is very rare in the studied deposit (Chovan et al., 2016[b]) and its presence has not been repeteadly confirmed. Se content in studied phases (~ 0.6 *apfu*) corresponds to mixed phase between galena and clausthalite, probably related to low fSe_2 in hydrothermal system. Similar transitional phases were determined at the Kremnica epithermal Au-Ag deposit (Števko et al., 2018).

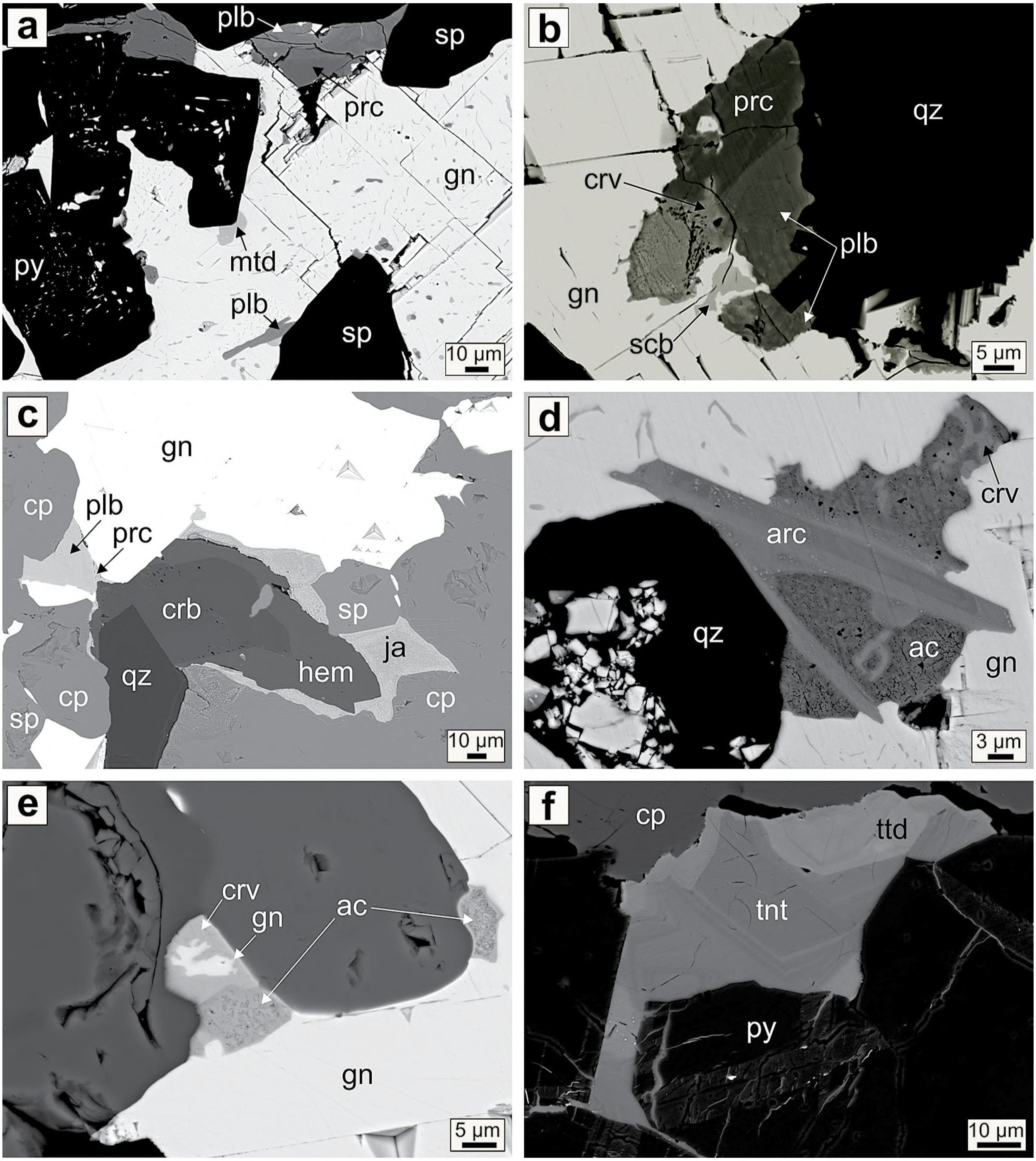

Fig. 10. Back-scattered electron images of Ag-(Bi, Cu, Sb, As)-S assemblage in horst-related veins. (a) Grains of polybasite, pearceite, and matildite in galena. Associated minerals are sphalerite and pyrite; (b) Intergrowth of polybasite, pearceite, cervelleite, and schapbachite in galena; (c) Polybasite, pearceite and jalpaite in galena. Associated minerals are sphalerite, chalcopyrite, hematite, quartz, and carbonate; (d) Intergrowth of needle-like arcubisite, cervelleite and acanthite, together in galena; (e) Intergrowth of acanthite and cervelleite in galena; (f) Intergrowth of tetrahedrite and tennantite in association with pyrite and chalcopyrite. Abbreviations: ac – acanthite; arc – arcubisite; cp – chalcopyrite; crb – carbonate; crv – cervelleite; gn – galena; hem – hematite; ja – jalpaite; mtd – matildite; plb – polybasite; prc – pearceite; py – pyrite; scb – schapbachite; sp – sphalerite; tnt – tennantite; ttd – tetrahedrite; qz – quartz.

The existence of a complete isomorphous series PbS-PbSe in natural samples was recently confirmed in the historic Krušné hory and Kutná Hora ore districts (Sejkora & Škácha, 2015; Sejkora et al., 2017; Pažout et al., 2019). During our study only low concentrations of Se (up to 0.06 *apfu*) were determined in petzite from LANF veins. The Se content in galena was not determined during previous study in the eastern part of the deposit (Kubač et al., 2018[a]).

Calaverite, krennerite, sylvanite, unnamed AgAuTeS phase, uytenbogaardtite, and petrovskaite are very rare minerals and were found in samples of flotation concentrates. They typically form separate isometric and irregular grains intergrowing with gold in sulphides and tellurides, and also reaction rims on the boundary of the gold grains. This mineral assemblage has not been determined yet in hand specimens on studied deposit. The presence of unidentified AgAuS mineral phases was also determined in sample of grinded ore (before ore-dressing process) using QEMSCAN Particle Mineral Analysis measurement (Chovan et al., 2016[a]). Presence of Au-Ag sulphides similar to uytenbogaardtite and petrovskaite was determined by Jeleň et al. (2018) in Natália vein in the western part of the deposit in previously collected samples. Au-Ag tellurides calaverite, krennerite, and sylvanite represent three end-members in Au-Ag-Te system, and are distinguished by Au↔Ag substitution in crystal structure (Dye & Smyth, 2012). These minerals typically replace gold grains according to reaction boundaries between them and gold. The replacement is manifested by formation of calaverite/sylvanite/krennerite, unnamed AgAuTeS phase, petzite with higher Ag content and hessite with higher Au content.

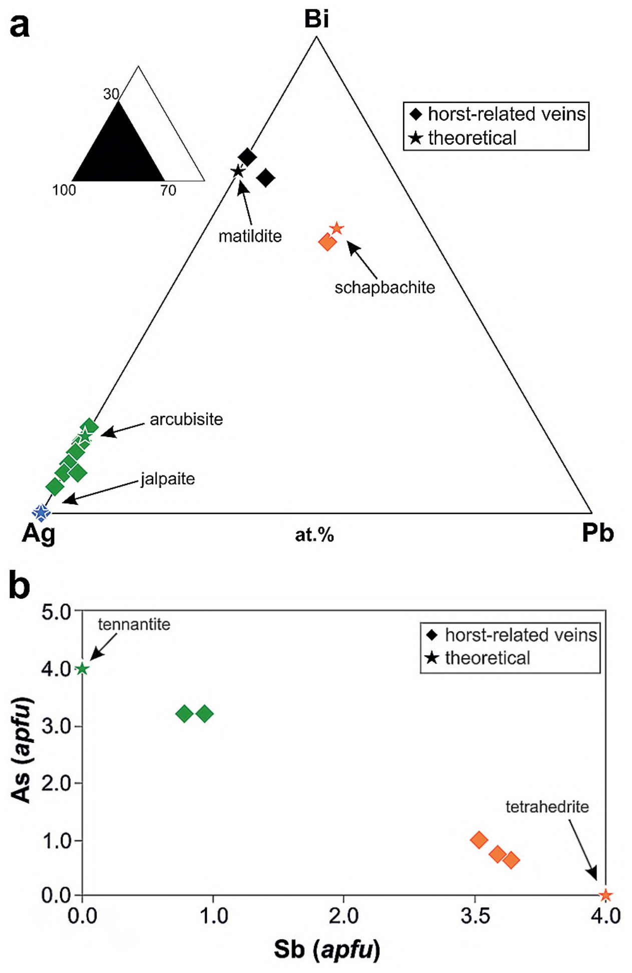

Fig. 11. A triangular Bi-Ag-Pb (a) and Sb vs. As (b)plot diagrams illustrating composition of minerals of Ag-(Bi, Cu, Sb, As)-Sassemblage in samples of horst-related veins from Banská Hodruša deposit. All data from EPMA analyses.

Uytenbogaardtite and petrovskaite typically form thin rims around aggregates of gold and tellurides. Crystallization of these high-temperature phases similar to $(Ag_{11}Au)Te_6$ was probably caused due to replacement of gold by Te- and Ag-rich fluids. According to Čvileva et al. (1988) the high-temperature $(Ag_{11}Au)Te_6$ phase may breakdown at temperatures below 50°C and mineral assemblage sylvanite-petzite-hessite or hessite-petzite could be formed. The reaction of Ag-, Te-, and S-rich fluids with gold probably generated the mineral association krennerite-sylvanite plus γ- and χ-phase (Zhai & Liu, 2014), which was breakdown to calaverite-krennerite-sylvanite-petzite or hessite-altaite assemblage after cooling. Cook et al. (2009) mentioned that gold-calaverite assemblage may represents eutectic assemblage at 400°C. However, at the temperatures below 200°C the gold-calaverite-petzite mineral assemblage is stable. Order of precipitation of minerals (calaverite-hessite-petzite and Ag-sulphides at the final stages) in this assemblage also supports the decreasing the fugacity fTe_2 (Afifi et al., 1988[b]). In recent work of Pal'yanova et al. (2014) the phenomenon of sulphidation of gold-electrum is often mentioned, where acanthite, uytenbogaardtite, and petrovskaite can be developed on the surface (often as intergrownths). According to thermodynamic calculations of Pal'yanova et al. (2016) the uytenbogaardtite and petrovskaite are formed at decreasing temperature (180 – 100°C) and fugacity fS_2, and at reduction→oxidation condition change in the environment. In the vicinity of Hodruša-Hámre village uytenbogaardtite was found as rims around electrum or as aggregates with acanthite at the locality of Rabenstein (Majzlan, 2009). Berkh et al. (2014) described the Se- and Te-rich uytenbogaardtite at Banská Belá and Kopanice settlements. Majzlan et al. (2018) found the uytenbogaardtite and petrovskaite at Nová Baňa town in association with acanthite in the form of corrosion haloes around electrum, formed at the final stage of mineralization. At the Rozália mine the occurence of these minerals is very rare and probably related to increasing the fS_2/fTe_2 ratio and decreasing the temperature in the final stage of mineralizing process. Due to very rare occurrence of this mineral assemblage within the both parts of the deposit the crystallization could be related to processes of ore-dressing plant. However, the process of such formation within the dressing plant environment is unknown. The formation of hypergenic Au-Ag sulphides and native gold in the presence of acanthite, pyrite, and other sulphides is possible in the reaction of gold-electrum with O_2- and CO_2-saturated surface waters at 25°C and 1 bar (Savva & Pal'yanova, 2007). However, the formation of Au-Ag tellurides is not described in this process.

Dominant form of tellurium transfer in fluid is $HTe^{-}_{(aq)}$, the transport of Te is supposed mostly as the gaseous phase. Telluride minerals (especially hessite) are formed by condensation of Te-bearing magmatic volatiles. During intensive boiling, tellurium is released to vapor, while precipitation of Au-Ag tellurides occurs during subsequent condensation of the vapor in ore-bearing fluids that transport gold (Cooke & McPhail, 2001). Therefore, during continuous boiling of fluids, precipitation of tellurides occurs simultaneously or after crystallization of gold. Temperatures of hessite precipitation are usually below 250°C, and if fTe_2 is rising the altaite and calaverite may be formed. Assemblage gold-acanthite will be dominant at low fTe_2/fS_2

ratio in fluid as it is mentioned in various works discussing about horst-related veins in the vicinity of Hodruša-Hámre and Nová Baňa sites (Berkh et al., 2014; Majzlan et al., 2016, 2018 and references therein).

In horst-related veins sampled in the eastern part of the Banská Hodruša deposit the increasing in Ag and sometimes Bi content was determined, while the Au, Te, and Se content is low or none. These elements are contained in sulphosalts, which intergrowth with base metal sulphides or create characteristic myrmekite textures with galena. The most of silver occurs in acanthite and polybasite/pearceite. Cervelleite is significant Ag-bearing mineral and also has relatively small amounts of Te in the studied samples. Low Te content occurs in acanthite, arcubisite, and pearceite. Jalpaite is very rare. The most significant Bi-bearing minerals in studied samples are matildite and schapbachite. Arcubisite has lower values of Bi content. The Se contents are usually low, only slight increase was found in cervelleite, acanthite, and some other sulphosalts. Selenium minerals have not been identified in this type of veins. The presence of described Ag-sulphides was previously determined in the Rozália horst-related vein in the western part of the deposit at the depth levels of LANF veins occurence (Koděra et al., 2005 and references therein). Bismuth mineralization is usually formed at higher temperatures in deeper levels as it is described in the Rozália mine by previous authors (Koděra et al., 1970; Jeleň et al., 2012; Sejkora et al., 2015). According to fluid inclusion data of Kovalenker et el. (1991) the bismuth mineralization is deposited at temperatures between 345 and 300°C and due to late gradual cooling and breakdown of primary high-temperature phases.

The most common mineral, which typically forms the largest grains, is polybasite-pearceite. This mineral was previously described in the horst-related veins by various authors and is considered to be a common Ag-bearing mineral (Koděra ed., 1986; Koděra et al., 2005). Tetrahedrite-tennantite is rare in veins of this type (Koděra ed., 1986). Polybasite/pearceite, acanthite, cervelleite, arcubisite, schapbachite, and matildite (most common) typically occur within the myrmekite aggregates with galena. Acanthite is formed by transition from high-temperature argentite at temperatures below 173°C (http://rruff.info/ima). Solid solution between matildite and galena is stable at temperatures above 215°C and below this temperature the characteristic exsolution textures are formed. Synthetic, low-temperature $AgBiS_2$ is stable at temperatures below 195°C (https://www.mindat.org/min-2592.html). Arcubisite with Ag_4TeS mineral phase was described for the first time in matildite- and aikinite-bearing galena within the cryolite deposit at Ivigtut, South Greenland (Karup-Møller, 1976). The minerals are considered to have crystallized contemporaneously with the galena host at temperatures below 230°C and at a pressure of around 2000 bars. According to fluid inclusion data of Koděra et al. (2005) from the horst-related Rozália vein, the two obtained maximal homogenization temperatures (at around 285°C and 187°C) probably corresponds to earlier and late stage of mineralization. Homogenization temperatures below 200°C suggest the possibility of cooling of the system and formation of exsolution textures.

6. CONCLUSIONS

Ag-Au tellurides and sulphosalts from epithermal Au-Ag-Pb-Zn-Cu deposit Banská Hodruša at the Rozália mine were found in two mineral assemblages.

The first Au-Ag-Te-S assemblage occurs in earlier veins related to low-angle normal fault shear zone (LANF) and it is represented by hessite, petzite, and gold/electrum as main minerals. Te-polybasite, Cu-cervelleite, altaite, and unnamed AgPbTeS mineral are rare. The same assemblage was determined in samples of flotation concentrates. However, in this assemblage the Au-Ag tellurides calaverite-krennerite-sylvanite are dominant in association with Au-hessite, petzite, unnamed AgAuTeS phase, uytenbogaardtite, and petrovskaite. Frequently occurring Au-Ag tellurides together with gold was probably deposited after boiling of fluids at temperatures of about 250°C, and at the high fugacity $f Te_2$. The multiphase assemblage described in the text was formed by the breakdown of high-temperature phase during cooling and change of the $f Te_2/f S_2$ ratio.

The second Ag-(Bi, Cu, Sb, As)-S assemblage was found in samples of younger horst-related veins. The main mineral in this assemblage is polybasite-pearceite, tetrahedrite-tennantite, the other minerals matildite, acanthite, schapbachite, cervelleite, and arcubisite are rare and typically form myrmekite texture with galena. Jalpaite may also occur in this assemblage. Silver and some other elements were divided to Ag-sulphosalts (polybasite-pearceite) or to high-temperature sulphides, mainly to Ag(Bi)-bearing galena. The high-temperature phases were breakdown to galena, matildite and other phases at temperatures below 200°C, typically with characteristic exsolution textures.

Acknowledgment: This study was supported by Slovenská Banská, Ltd., Slovak Research and Development Agency (contract No. APVV-15-0083), and the Research Agency of the Ministry of Education, Science, Research and Sport of the Slovak Republic (contract No. VEGA 1/0560/15). Authors are thankful to Jiří Sejkora and Martin Števko for the constructive review, and to journal editor Jaroslav Pršek for the editorial handling.

References

Afifi A.M., Kelly W.C. & Essene E.J., 1988[a]: Phase relations among tellurides, sulphides, and oxides: I. Thermochemical data and calculated equilibria. *Economic Geology*, 83, 377–394.

Afifi A.M., Kelly W.C. & Essene E.J., 1988[b]: Phase relations among tellurides, sulphides, and oxides: II. Applications to telluride-bearing ore deposits. *Economic Geology*, 83, 395–404.

Alderton D.H.M. & Fallick E.J., 2000: The nature and genesis of gold-silver-tellurium mineralization in the Metaliferi Mountains of Western Romania. *Economic Geology*, 95, 495–516.

Bakos F., Chovan M., Žitňan P. (Eds.), Bačo P., Bahna B., Bednárová S., Bednár R., Ferenc Š., Finka O., Gargulák M., Hrašková E., Hvožďara P., Jeleň S., Kamhalová M., Kaňa R., Knesl J., Križáni I., Labuda J., Lalinský T., Maťo Ľ., Miklovič J., Mikuš T., Ondrus P., Pauditš P., Soják M., Sombathy L.,Šály J., 2017: Gold in Slovakia. Lúč, Bratislava, 429 p.

Berkh K., Majzlan J., Chovan M., Kozák J. & Bakos F., 2014: Mineralogy of the Medieval Au-Ag occurrences Banská Belá, Treiboltz, Rabenstein, and Kopanice in the Banská Štiavnica ore district (Slovakia). *Neues Jahrbuch fur Mineralogie – Abhandlungen*, 33, 4, 329–347.

Cabri L.J., 1965: Phase relations in the Au-Ag-Te system and their mineralogical significance. *Journal of Economic Geology*, 60, 1569–1606.

Chernyshev I.V., Konečný V., Lexa J., Kovalenker V.A., Jeleň S., Lebedev V.A. & Goltsman Y.V., 2013: K-Ar and Rb-Sr geochronology and evolution of the Štiavnica Stratovolcano (Central Slovakia). *Geologica Carpathica*, 64, 327–351.

Chovan M., Jágerský I., Delaney V., Žitňan P., Kubač A., Bačík P., Troppová D. & Mikuš T., 2016[a]: Mineralogy of Au (Ag, Pb, Cu) ore dressing products from Banská Hodruša epithermal deposit. *Acta Geologica Slovaca*, 8, 203–216.

Chovan M., Kubač A., Jágerský I., Žitňan P., Prcúch J., Okáľ M., Mikuš T., Troppová D., Bačík P., Brčeková J., Voleková B., Koděra P. & Števko M., 2016[b]: Mineralógia hydrotermálnych žíl a produktov úpravy rúd Au (Ag, Pb, Cu) ložiska Banská Hodruša. [Mineralogy of hydrothermal veins and dressing products from Banská Hodruša Au(Ag,Pb,Cu) deposit]. Manuscript, KMP PRIF UK archive, Comenius University, Bratislava, 206 p. [in Slovak]

Ciobanu C.L., Cook N.J. & Spry P.G., 2006: Preface-special issue: telluride and selenide minerals in gold deposits-how and why? *Mineralogy & Petrology*, 87, 163–169.

Cook N.J. & Ciobanu C.L., 2003: Cervelleite, Ag_4TeS from three localities in Romania, substitution of Cu, and the occurrence of the associated phase, Ag_2Cu_2TeS. *Neues Jahrbuch für Mineralogie – Monatshefte*, 7, 321–336.

Cook N.J., Ciobanu C.L., Damian G. & Damian F., 2004: Tellurides and sulphosalts from deposits in the Golden Quadrilateral. IAGOD Guidebook Series, 12, 111–144.

Cook N.J., Ciobanu C.L., Spry P.G. & Voudoris P., 2009: Understanding gold-(silver)-telluride-(selenide) mineral deposits. *Episodes*, 32, 249–263.

Cooke D.R. & McPhail D.C., 2001: Epithermal Au-Ag-Te mineralization, Acupan, Baguio district, Philippines: Numerical simulations of mineral deposition. *Economic Geology*, 96, 109–131.

Čvileva T.N., Bezsmertnaja M.M. & Spiridonov M., 1988: Spravocnik – opredelitel rudnich mineralov v otrazennom svete. [Manual for the determination of ore minerals in reflected light]. Nedra, Moscow, 504 p. [in Russian]

Dye M.D. & Smyth J.R., 2012: The crystal structure and genesis of krennerite, Au_3AgTe_8. *The Canadian Mineralogist*, 50, 363–371.

Gavora S., 1988: Dokumentácia vrtu BLI-6 v mierke 1:100. [Drill log of the BLI-6 drill-hole in the 1:100 scale]. Open file report, archive ŠGÚDŠ Bratislava, 30 p.[in Slovak]

Grancea L., Bailly L., Leroy J., Banks D., Marcoux E., Milési J.P., Cuney M., André A. S., Istvan D. & Fabre C., 2002: Fluid evolution in the Baia Mare epithermal gold/polymetallic district, Inner Carpathians, Romania. *Mineralium Deposita*, 37, 630–647.

Hough R.M., Butt C.R.M. & Fischer-Bühmer J., 2009: The crystallography, metallography and composition of Au. *Elements*, 5, 297–302.

Jeleň S. & Háber M., 2000: Mineralógia mineralizácií bane Rozália, Hodruša-Hámre. [Mineralogy of the Rozália mine mineralization types, Hodruša-Hámre]. Open file report. Geological Survey of Slovak Republic, Bratislava, 78 p.[in Slovak]

Jeleň S., Maťo Ľ., Koděra P. & Kovalenker V.A., 2004: Se-Te mineralogy of Neogene epithermal deposits and occurrences of Slovakia. IAGOD Guidebook Series, 12, 230–231.

Jeleň S., Pršek J., Kovalenker V.A., Topa D., Sejkora J., Števko M. & Ozdín D., 2012: Bismuth sulfosalts of the cuprobismutite, pavonite and aikinite series from the Rozália mine, Hodruša-Hámre, Slovakia. *The Canadian Mineralogist*, 50, 325–340.

Jeleň S., Kurylo S., Kovalenker V.A., Luptáková J., Poľák Ľ. & Durajová R., 2018: New data on chemical composition of Au-Ag-S system minerals in precious and base metal deposit Hodruša-Hámre. Proceedings of the Central-European Mineralogical Conference, Comenius University, Bratislava, p. 39.

Karup-Møller S., 1976: Arcubisite and mineral B – two new minerals from the cryolite deposit at Ivigtut, south Greenland. *Lithos*, 9, 4, 253–257.

Koděra M., 1963: Gesetzmässigkeinten der zonalen Verteilung der Mineralisation in der subvulkanischenpolymetallischen Lagerstätte Banská Štiavnica. [Principles of the zonal distribution of the mineralization at the subvolcanic polymetallic deposit Banská Štiavnica]. In: Symposium: Problems of Postmagmatic Ore Deposition. Geological Survey of Czech Republic, Prague, 1, 184–189. [in German]

Koděra M. (Ed.), 1986: Topographic mineralogy of Slovakia. VEDA, Bratislava, 1590 p. [in Slovak with English preface and introduction]

Koděra M., Kupčík V. & Makovicky E., 1970: Hodrushite – a new sulphosalt. *Mineralogical Magazine*, 37, 641–648.

Koděra P. & Lexa J., 2010: Classic localities in Central Slovakia Volcanic Field: Gold, silver and base metal mineralizations and mining history at Banská Štiavnica and Kremnica. *Acta Mineralogica-Petrographica*, Field Guide Series, 29, 1–19.

Koděra P., Lexa J. & Rankin A. H., 2005: Epithermal gold veins in a caldera setting: Banská Hodruša, Slovakia. *Mineralium Deposita*, 39, 921–943.

Konečný V., Lexa J. & Hojstričová V., 1995: The Central Slovakia Neogene Volcanic Field: a review. *Acta Vulcanologica*, 7, 63–78.

Kovalenker V.A., Jeleň S., Levin K.A., Naumov V.B., Prokofjev V.J. & Rusinov V.L., 1991: Mineral assemblages and psychical-chemical model of the formation of gold-silver-polymetallic mineralization on the deposit Banská Štiavnica (Central Slovakia). *Geologica Carpathica*, 42, 291–302.

Kubač A., Chovan M., Koděra P., Kyle J.R., Žitňan P., Lexa J. & Vojtko R., 2018[a]: Mineralogy of the epithermal precious and base metal deposit Banská Hodruša at the Rozália Mine (Slovakia). *Mineralogy & Petrology*, 112, 705–731.

Kubač A., Koděra P., Uhlík P., Fallick A. E., Chovan M. & Vojtko R., 2018[b]:Genetické aspekty epitermálnej drahokovovo-polymetalickej mineralizácie na ložisku Banská Hodruša. [Genetical aspects of the epithermal precious-base metal mineralization at the Banská Hodruša deposit]. Proceedings of the conference Geochémia 2018, State Geological Institute of Dionýz Štúr in Bratislava, pp. 80–83[in Slovak]

Lexa J., Štohl J. & Konečný V., 1999: Banská Štiavnica ore district: relationship among metallogenetic processes and geological evolution of a stratovolcano. *Mineralium Deposita*, 34, 639–665.

Majzlan J., 2009: Ore mineralization at the Rabenstein occurrence near Banská Hodruša, Slovakia. *Mineralia Slovaca*, 41, 45–54.

Majzlan J., Berkh K., Koděra P., Števko M., Bakos F. & Milovský R., 2016: A mineralogical, fluid inclusion, and isotopic study of selected epithermal Ag-Au occurrences in the Banská Štiavnica-Hodruša-Hámre ore district, Western Carpathians. *Acta Geologica Slovaca*, 8, 2, 133–147.

Majzlan J., Berkh K., Kiefer S., Koděra P., Fallick A. E., Chovan M., Bakos F., Biroň A., Ferenc Š. & Lexa J., 2018: Mineralogy, alteration patterns, geochemistry, and fluid properties of the Au-Ag epithermal deposit Nová Baňa, Slovakia. *Mineralogy & Petrology*, 111, 1–23.

Maťo Ľ., Sasvári T., Bebej J., Kraus I., Schmidt R. & Kalinaj M., 1996: Structurally-controlled vein-hosted mezothermal gold-quartz and epithermal precious and base metal mineralization in the Banská Hodruša ore field, Central Slovakia neovolcanites. *Mineralia Slovaca*, 28, 455–490 [in Slovak with English resume]

Pal'yanova G.A., Karnanov N. & Savva N.E., 2014: Sulfidation of native gold. *American Mineralogist*, 99, 1095–1103.

Pal'yanova G.A., Savva N.E., Zhuravkova T.V. & Kolova E.E., 2016: Gold and silver minerals in low-sulfidation ores of the Julietta deposit (northeastern Russia). *Russian Geology & Geophysics*, 57, 1171–1190.

Pals D. & Spry P., 2003: Telluride mineralogy of the low-sulfidation epithermal Emperor gold deposit, Vatukoula, Fiji. *Mineralogy &Petrology*, 79, 285–307.

Pažout R., Sejkora J. & Šrein V., 2019: Ag-Pb-Sb sulfosalts and Se-rich mineralization of Anthony of Padua Mine near Poličany – Model example of the mineralization of silver lodes in the historic Kutná Hora Ag-Pb ore district, Czech Republic. *Minerals*, 9, 430, 1–44.

Pietruszka D.K., 2016: Gold-base metal mineralization from the Hodruša-Rozália mine, Slovakia. MSc. diploma thesis, archive of AGH, Krakow, 65 p.

Savva N.E.& Pal'yanova G.A., 2007: Genesis of gold and silver sulfides at the Ulakhan deposit (northeastern Russia). *Russian Geology and Geophysics*, 48, 799–810.

Sejkora J. & Škácha P., 2015: Selenides from fluorite deposit at Moldava in the Krušné hory Mts. Czech Republic. *Bulletin mineralogicko-petrologického Oddělení Národního Muzea (Praha)*, 23, 229–241. [in Czech]

Sejkora J., Števko M., Ozdín D., Pršek J. & Jeleň S., 2015: Unusual morphological forms of hodrušite from the Rozália vein, Hodruša-Hámre near Banská Štiavnica (Slovak Republic). *Journal of Geosciences*, 60, 11–22.

Sejkora J., Šrein V., Šreinová B. & Dolníček Z., 2017: Selenide mineralization of the uranium deposit Potůčky in the Krušné hory Mts. (Czech Republic). *Bulletin mineralogicko-petrologického Oddělení Národního Muzea (Praha)*, 25, 306–317. [in Czech]

Sillitoe R.H., 2002: Some metallogenic features of gold and copper deposits related to alkaline rocks and consequences for exploration. *Mineralium Deposita*, 37, 4–13.

Simmons S.F., White N.C. & John D.A., 2005: Geological characteristics of epithermal precious and base metal deposits. Economic Geology 100th Anniversary Volume, pp. 485–522.

Shackleton J.M., Spry P.G. & Baterman R., 2003: Telluride mineralogy of the golden mile deposit, Kalgoorlie, Western Australia. *The Canadian Mineralogist*, 41, 1503–1524.

Spry P., Foster F., Truckle J. & Chadwick T., 1997: The mineralogy of the Golden Sunlight gold-silver telluride deposit, Whitehall, Montana, USA. *Mineralogy & Petrology*, 59, 143–164.

Šály J., Biroň A., Hók J., Lepeň I., Kámen M., Prcúch J. & Reck V., 2003:Komplexné zhodnotenie zatvoreného ložiska Au, Ag – Hodruša. [Complex evaluation of the closed Au, Ag deposit Hodruša]. Open file report,archiveŠGÚDŠ Bratislava, 95 p.[in Slovak]

Šály J., Hók J., Lepeň I., Okáľ M., Reck V. & Varga P., 2008:Vyhľadávanie telies s drahokovovým zrudnením v okolí ložiska Hodruša-Svetozár. [Exploration of bodies with precious metal mineralization in the vicinity of the deposit Hodruša-Svetozár]. Final report with calculation of reserves. Confidential report,archive ŠGÚDŠ Bratislava, 85 p.[in Slovak]

Števko M., Sejkora J. & Macek I., 2015: Unusual morphological type of gold from the Rozália mine, Hodruša-Hámre (Slovak Republic). *Bulletin mineralogicko-petrologického Oddělení Národního Muzea (Praha)*, 23, 1, 26–29. [in Slovak]

Števko M., Sejkora J., Dolníček Z. & Škácha P., 2018: Selenium-rich Ag-Au Mineralization at the Kremnica Au-Ag epithermal deposit, Slovak Republic. *Minerals*, 8, 572, 1–26, doi:10.3390/min8120572

Vojtko R., Žitňan P., Prcúch J., Lexa J., Chovan M., Koděra P. & Kubač A., 2018: Structure of the epithermal Au-Ag deposit of Banská Hodruša (Štiavnica stratovolcano, Western Carpathians). Proceedings of the conference ESSEWECA, Comenius University, Bratislava, pp. 130–131.

Voudoris P.C., Spry P.G., Sakellaris G.A. & Mavrogonatos C., 2011: A cervelleite-like mineral and other Ag-Cu-Te-S minerals in gold-bearing veins in metamorphic rock of the Cycladic Blueschist Unit, Kallianou, Evia Island, Greece. *Mineralogy & Petrology*, 101, 169–183.

Wallier S., Rey R., Kouzmanov K., Pettke T., Heinrich C.A., Leary S., O'Connor G., Tămaş C.G., Vennemann T. & Ullrich T., 2006: Magmatic fluids in the breccia-hosted epithermal deposit of Roşia Montană, Romania. *Economic Geology*, 101, 923–954.

Xu H., Yu Y.X., Wu X.K., Yang L.J., Tian Z., Gao S. & Wang Q.S., 2012: Intergrowth texture in Au-Ag-Te minerals from Sandaowanzi gold deposit, Heilongjiang Province: Implications for ore-forming environment. *Chinese Science Bulletin*, 57, 2778–2786.

Zhai D. & Liu J., 2014: Gold-telluride-sulfide association in the Sandaowanzi epithermal Au-Ag-Te deposit, NE China: implications for phase equilibrium and physicochemical conditions. *Mineralogy &Petrology*, 108, 853–871.

http://rruff.info/ima

https://www.mindat.org/min-2592.html